AD_____

Award Number: DAMD17-02-1-0418

TITLE: Role of the Neddylation Enzyme Uba3, a New Estrogen Receptor Corepressor, in Breast Cancer

PRINCIPAL INVESTIGATOR: Kenneth P. Nephew, Ph.D.

CONTRACTING ORGANIZATION: Indiana University
Indianapolis, IN 46202-5167

REPORT DATE: September 2005

TYPE OF REPORT: Annual Summary

PREPARED FOR: U.S. Army Medical Research and Materiel Command
Fort Detrick, Maryland 21702-5012

DISTRIBUTION STATEMENT: Approved for Public Release;
Distribution Unlimited

The views, opinions and/or findings contained in this report are those of the author(s) and should not be construed as an official Department of the Army position, policy or decision unless so designated by other documentation.

20060110 087

REPORT DOCUMENTATION PAGE

Form Approved
OMB No. 0704-0188

1. REPORT DATE (DD-MM-YYYY)	2. REPORT TYPE	3. DATES COVERED (From - To)
01-09-2005	Annual Summary	1 Sep 2004 – 31 Aug 2005

4. TITLE AND SUBTITLE

Role of the Neddylation Enzyme Uba3, a New Estrogen Receptor Corepressor, in Breast Cancer

5a. CONTRACT NUMBER

5b. GRANT NUMBER
DAMD17-02-1-0418

5c. PROGRAM ELEMENT NUMBER

6. AUTHOR(S)
Kenneth P. Nephew, Ph.D.

E-mail: knephew@indiana.edu

5d. PROJECT NUMBER

5e. TASK NUMBER

5f. WORK UNIT NUMBER

7. PERFORMING ORGANIZATION NAME(S) AND ADDRESS(ES)

Indiana University
Indianapolis, IN 46202-5167

8. PERFORMING ORGANIZATION REPORT NUMBER

9. SPONSORING / MONITORING AGENCY NAME(S) AND ADDRESS(ES)
U.S. Army Medical Research and Materiel Command
Fort Detrick, Maryland 21702-5012

10. SPONSOR/MONITOR'S ACRONYM(S)

11. SPONSOR/MONITOR'S REPORT NUMBER(S)

12. DISTRIBUTION / AVAILABILITY STATEMENT
Approved for Public Release; Distribution Unlimited

13. SUPPLEMENTARY NOTES

14. ABSTRACT
Estrogens play important roles in both the onset and malignant progression of breast cancer. The content of estrogen receptors in breast tumors is a valuable predictor of whether a patient will respond to therapy with antiestrogens, such as tamoxifen and fulvestrant (ICI 182,780). Expression and activity of ER can be lost or impaired in antiestrogen-resistant breast cancer. The proposed studies are designed to test the overall hypothesis that the ubiquitin-like NEDD8 protein modification pathway represses estrogen action by facilitating degradation of ER protein. Perturbation of this pathway may prove instrumental in breast tumor progression; alternatively, activation of this pathway may prove to be a valid target for novel therapeutics. This study on mechanisms that regulate ER levels and activity are highly relevant to the development and progression breast cancer, including tumor progression to states of hormone independence and antiestrogen resistance. Thus, understanding how the estrogen receptor is regulated is an area of research critical to understanding the tissue selective pharmacology of estrogens. In addition, tamoxifen and other selective estrogen receptor modulators target the estrogen receptor, and this study is of the utmost relevance to those important therapies.

15. SUBJECT TERMS
Estrogen receptor, corepressor, ubiquitination, nuclear receptors, transcription

16. SECURITY CLASSIFICATION OF:			17. LIMITATION OF ABSTRACT	18. NUMBER OF PAGES	19a. NAME OF RESPONSIBLE PERSON
a. REPORT	b. ABSTRACT	c. THIS PAGE			19b. TELEPHONE NUMBER (include area code)
U	U	U	UU	67	

Standard Form 298 (Rev. 8-98)
Prescribed by ANSI Std. Z39.18

Table of Contents

INTRODUCTION

Estrogen regulates diverse biological processes through estrogen receptors (ERα and ERβ) (1). Receptor levels and dynamics have a profound influence on target tissue responsiveness and sensitivity to estrogen, and receptor turnover rates provide estrogen target cells with the capacity for rapid regulation of receptor levels and thus dynamic hormone responses (2-5). Furthermore, several experimental results have recently demonstrated that receptor degradation is a key component of the response of cancer cells, including breast cancer cells, to antiestrogen therapy (6, 7). In advanced stage breast cancers, estrogen receptor expression and activity can be lost or impaired, and the tumors are often resistant to endocrine therapies, such as the steroidal antiestrogens, ICI 182,780 and ICI 164,384 (6, 7). Our findings during the funding period have raised the intriguing possibility for a role of ubiquitin and ubiquitin-like pathways, including the NEDD8 pathway, in ERα ubiquitination and degradation and suggest that disruptions in such pathways may contribute to the development of antiestrogen-resistance in human breast cancer. The overall hypothesis that ubiquitin protein modification pathways repress estrogen action by facilitating degradation of ER protein was tested. Our experimental results suggest that perturbation of this pathway may prove instrumental in breast tumor progression; alternatively, activation of ubiquitin protein modification pathways may prove to be valid targets for novel therapeutics.

BODY

Task 1 was to determine the effect of Uba3 on breast cancer cell proliferation. We attempted to generate breast cancer cell lines stably expressing During the past year, we attempted to use an inducible promoter to control expression levels of the dominant negative Uba3 (C216S), a mutant that we had used previously to block the NEDD8 pathway (8). These efforts were unsuccessful, as blocking this pathway in MCF7 breast cancer cells turned out to be lethal. We conclude that the NEDD8 is essential for cell survival. Task one has been completed.

The second task of the project was to determine the molecular mechanisms of ERα corepression by the NEDD8 pathway. During the funding period, we generated point mutations within the nuclear receptor interacting motifs (the NR boxes) of Uba3 and then proposed to examine direct interactions of the mutant proteins with ER. Constructs were made and sequenced. However, we were unable to express proteins from the new constructs, for reasons that are unclear at this time. We speculate that perhaps the mutations made the protein unstable. Nonetheless, although mostly negative results were obtained, Task 2 has been completed.

Task 3 was to determine if ERα and ERα function is modified by APP-BP1 and Ubc12 and an NEDD8 target protein. As described in previous annual reports, task 3 has been completed, and we have continued to perform further investigations into the roles of ubiquitin-like pathway NEDD8 in the responses to estradiol and antiestrogens (deemed a logical extension of the SOW and within the scope of the fundamental questions underlying the SOW). Thus, we continued to investigate the role of the ubiquitin-proteasome pathway in ERα-mediated transcriptional responses in breast cancer cells.

Abnormal expression of ERα has long been associated with both the initiation and progression of breast cancer (10). An increase in the number of ERα-positive cells, as well as increased individual cell ERα content, have frequently been detected in malignant breast tumors (11). Furthermore, increased ERα content has been shown to augment the magnitude of estrogen-stimulated gene expression, providing a growth advantage to breast cancer cells (2, 8, 9,12). Collectively, these observations indicate that alterations in ERα degradation pathways may contribute to deregulation of ERα, perhaps leading to enhanced estrogen action in breast tumors.

We and others have clearly shown degradation of unliganded ERα is mediated by the ubiquitin-proteasome pathway, regulation of this pathway, at the molecular level, remains unclear. One potential mechanism involves CHIP, the carboxyl terminus of Hsc70-interacting protein, previously shown to target Hsp90 interacting proteins for ubiquitination and proteasomal degradation. We investigated a role for CHIP in degradation of unliganded ERα (13; manuscript attached). In HeLa cells transfected with ERα and CHIP, ERα is downregulated through a ubiquitination dependent pathway, while ERα-mediated gene transcription decreased (Fig. 1 and Fig 2A). In contrast, siRNA inhibition of CHIP expression resulted in increased ERα accumulation and reporter gene transactivation (Fig 1B and Fig 2B). Transfection of mutant CHIP constructs demonstrated that both the U-box (containing ubiquitin ligase activity) and the tetratricopeptide repeat (TPR, essential for chaperone binding) CHIP domains are required for CHIP-mediated ERα downregulation (Fig 3). In addition, coimmunoprecipitation assays demonstrated that ERα and CHIP associate through the CHIP TPR domain (Fig 3). In ERα-positive breast cancer MCF7 cells, CHIP overexpression resulted in decreased levels of endogenous ERα protein and attenuation of ERα-mediated gene expression (Figs 4-6). Furthermore, ERα-CHIP interaction was induced by the Hsp90 inhibitor geldanamycin (GA), resulting in enhanced ER-alpha degradation; this GA effect was further enhanced by CHIP overexpression, but was abolished by CHIP-siRNA (Figs 7 & 8). Finally, ERα dissociation from CHIP by various ERα ligands, including estradiol, tamoxifen, and ICI 182,780 interrupted CHIP-mediated ERα degradation (Fig 9). These results demonstrate a role for CHIP in both basal and GA-induced ERα degradation. Furthermore, based on our observations that CHIP promotes ERα degradation and attenuates receptor-mediated gene transcription, we suggest that CHIP, by modulating ERα stability, contributes to the regulation of functional receptor levels, and thus hormone responsiveness, in estrogen target cells (summarized in Fig 11). Thus, based on our results, the chaperone/CHIP pathway, by

4

regulating ERα, levels, likely contributes to the development/progression of breast cancer. We believe that such a possible role for CHIP in breast cancer merits further examination.

In addition, during the funding period, we contributed to collaborative projects on the regulation of ER target genes in breast cancer, resulting in a co-authored publication (14; manuscript in appendix).

KEY RESEARCH ACCOMPLISHMENTS
- Demonstrated that CHIP promotes ERα degradation and attenuates receptor-mediated gene transcription.
- Provided evidence to suggest that CHIP, by modulating ERα stability, contributes to the regulation of functional receptor levels, and thus hormone responsiveness, in estrogen target cells.
- Provided evidence to suggest the chaperone/CHIP pathway, by regulating ERα, levels, may contribute to the development/progression of breast cancer.

REPORTABLE OUTCOMES
Manuscripts

1. *Fan M, Park A, **Nephew KP**. Interactions between estrogen receptor and the COOH terminus of the Hsp70-interacting protein (CHIP) (Mol Endocrinol, in press)
2. *Leu YW, Yan PS, Fan W, Jin VX, Liu CJ, Curran EM, Welshons WV, Wei HS, Davuluri RV, Plass C, **Nephew KP,** Huang TH-M. 2004. Loss of estrogen signaling triggers epigenetic silencing of downstream targets Cancer Res 64:8184-8192 (cover article).

*This DOD award is acknowledged in these publications.

Presentations
1. Fan M, Park A, **Nephew KP** 2005 CHIP (Carboxyl Terminus of Hsc70-Interacting Protein) promotes basal and geldanamycin-induced degradation of estrogen receptor-α. 87th annual Meeting of The Endocrine Society, San Diego, CA (platform talk).

CONCLUSIONS

The antiestrogen ICI 182,780 is a drug is used as a second-line endocrine agent in patients who have developed tamoxifen-resistant breast cancer. Despite its potent antitumor effects, the drug does not circumvent the development of antiestrogen resistance (15-17). Moreover, the fact that most tumors acquiring ICI 182,780 resistance do so while retaining expression of ERα and estrogen responsiveness (18-20), suggests that administration of the antiestrogen may possibly lead to the selection of tumor cells defective in ERα down-regulation pathway(s), which in turn may confer a proliferative advantage in either the presence or absence of estrogens. In this context, mechanism underlying persistent expression of ERα in tumors with acquired resistance, such as disruptions in the NEDD8, CHIP or other ubiquitin or ubiquitin-associated/protein receptor degradation pathways, may thus present an important therapeutic target for future drug intervention.

For the "so what section" (evaluates the knowledge as a scientific or medical product to also be included in the conclusion of this report), the loss of ERα degradation pathway(s) may provide a mechanism by which breast cancer cells acquire antiestrogen resistance while retaining expression of ERα. Pathways that utilize the ubiquitin-proteasome system could serve as a therapeutic targets for breast cancer.

List of personnel receiving pay from the research effort: Kenneth P. Nephew, Ph.D., Principal Investigator; Meiyun Fan, Ph.D., Postdoctoral Fellow; Teresa Craft, M.S., Research Associate, Annie Park, B.S., Research Associate, Xinghua Long, Graduate Student.

REFERENCES CITED

1. Barkhem T, Nilsson S, Gustafsson JA 2004 Molecular mechanisms, physiological consequences and pharmacological implications of estrogen receptor action. Am J Pharmacogenomics 4:19-28

2. Webb P, Lopez GN, Greene GL, Baxter JD, Kushner PJ 1992 The limits of the cellular capacity to mediate an estrogen response. Mol Endocrinol 6:157-67

3. Klinge CM 2000 Estrogen receptor interaction with co-activators and co-repressors. Steroids 65:227-51.

4. Reid G, Denger S, Kos M, Gannon F 2002 Human estrogen receptor-alpha: regulation by synthesis, modification and degradation. Cell Mol Life Sci 59:821-31

5. Eckert RL, Mullick A, Rorke EA, Katzenellenbogen BS 1984 Estrogen receptor synthesis and turnover in MCF-7 breast cancer cells measured by a density shift technique. Endocrinology 114:629-37

6. Dauvois S, Danielian PS, White R, Parker MG 1992 Antiestrogen ICI 164,384 reduces cellular estrogen receptor content by increasing its turnover. Proc Natl Acad Sci U S A 89:4037-41

7. Dauvois S, White R, Parker MG 1993 The antiestrogen ICI 182780 disrupts estrogen receptor nucleocytoplasmic shuttling. J Cell Sci 106:1377-88

8. Fan M, Bigsby RM, **Nephew KP** 2003 The NEDD8 pathway is required for proteasome mediated degradation of human estrogen receptor-α and essential for the antiproliferation activity of ICI 182,780 in ER-positive breast cancer cells Mol Endocrinol 17:356-365

9. Fan M, Nakshatri H, **Nephew KP**. 2004. Inhibiting proteasomal proteolysis sustains estrogen receptor-alpha activation. Mol Endocrinol 18:2603-2615

10. Anderson E 2002 The role of oestrogen and progesterone receptors in human mammary development and tumorigenesis. Breast Cancer Res 4:197-201

11. Sommer S, Fuqua SA 2001 Estrogen receptor and breast cancer. Semin Cancer Biol 11:339-52

12. Fowler AM, Solodin N, Preisler-Mashek MT, Zhang P, Lee AV, Alarid ET 2004 Increases in estrogen receptor-alpha concentration in breast cancer cells promote serine 118/104/106-independent AF-1 transactivation and growth in the absence of estrogen. Faseb J 18:81-93

13. Fan M, Park A, **Nephew KP**. Interactions between estrogen receptor and the COOH terminus of the Hsp70-interacting protein (CHIP) (Mol Endocrinol under revision)

14. Leu YW, Yan PS, Fan W, Jin VX, Liu CJ, Curran EM, Welshons WV, Wei HS, Davuluri RV, Plass C, **Nephew KP,** Huang TH-M. 2004. Loss of estrogen signaling triggers epigenetic silencing of downstream targets Cancer Res 64:8184-8192

15. Howell A, Osborne CK, Morris C, Wakeling AE 2000 ICI 182,780 (Faslodex): development of a novel, "pure" antiestrogen. Cancer 89:817-25

16. Lykkesfeldt AE, Larsen SS, Briand P 1995 Human breast cancer cell lines resistant to pure anti-estrogens are sensitive to tamoxifen treatment. Int J Cancer 61:529-34

17. Osborne CK, Coronado-Heinsohn EB, Hilsenbeck SG, Osborne CK, Coronado-Heinsohn EB, Hilsenbeck SG, McCue BL, Wakeling AE, McClelland RA, Manning DL, Nicholson RI 1995 Comparison of the effects of a pure steroidal antiestrogen with those of tamoxifen in a model of human breast cancer. J Natl Cancer Inst 87:746-50

18. Dumont JA, Bitonti AJ, Wallace CD, Baumann RJ, Cashman EA, Cross-Doersen DE 1996 Progression of MCF-7 breast cancer cells to antiestrogen-resistant phenotype is accompanied by elevated levels of AP-1 DNA-binding activity. Cell Growth Differ 7:351-9

19. Larsen SS, Heiberg I, Lykkesfeldt AE 2001 Anti-oestrogen resistant human breast cancer cell lines are more sensitive towards treatment with the vitamin D analogue EB1089 than parent MCF-7 cells. Br J Cancer 84:686-90.

20. Brunner N, Boysen B, Jirus S, Skaar TC, Holst-Hansen C, Lippman J, Frandsen T, Spang-Thomsen M, Fuqua SA, Clarke R 1997 MCF7/LCC9: an antiestrogen-resistant MCF-7 variant in which acquired resistance to the steroidal antiestrogen ICI 182,780 confers an early cross-resistance to the nonsteroidal antiestrogen tamoxifen. Cancer Res 57:3486-93

APPENDICES

Reprints:

1. Fan M, Park A, **Nephew KP.** Interactions between estrogen receptor and the COOH terminus of the Hsp70-interacting protein (CHIP) (Mol Endocrinol under revision)

2. Leu YW, Yan PS, Fan W, Jin VX, Liu CJ, Curran EM, Welshons WV, Wei HS, Davuluri RV, Plass C, **Nephew KP,** Huang TH-M. 2004. Loss of estrogen signaling triggers epigenetic silencing of downstream targets Cancer Res 64:8184-8192

CHIP (Carboxyl Terminus of Hsc70-Interacting Protein) Promotes Basal and Geldanamycin-Induced Degradation of Estrogen Receptor-alpha

Meiyun Fan[1], Annie Park[1], and Kenneth P. Nephew[1,2,3,4]

5   [1]Medical Sciences, Indiana University School of Medicine, Bloomington, IN 47405; [2]Indiana University Cancer Center; [3]Department of Cellular and Integrative Physiology, Indiana University School of Medicine, Indianapolis, IN 46202.

[4]To whom correspondence should be addressed:

                     Kenneth P. Nephew, Ph.D.
                     Medical Sciences
                     Indiana University School of Medicine
                     302 Jordan Hall
                     1001 E. 3rd St.
                     Bloomington, Indiana 47405-4401
                     Phone: (812) 855-9445
                     FAX: (812) 855-4436
                     E-mail:knephew@indiana.edu

Abbreviations: CHIP, carboxyl terminus of Hsc70-interacting protein; csFBS, dextran-coated

charcoal-stripped fetal bovine serum; DMSO, Methyl sulfoxide; E2, 17β-estradiol; ERα,

estrogen receptor-alpha; ERE, estrogen response element; GA, geldanamycin; GFP, green

fluorescence protein; HA, hemagglutinin; Hsp, heat shock protein; ICI, ICI 182,780; Luc, firefly

luciferase; OHT, 4-hydroxytamoxifen; siRNA, small interference RNA; TPR, tetratricopeptide

repeat.

ABSTRACT

In estrogen target cells, estrogen receptor-alpha (ERα) protein levels are strictly regulated. Although receptor turnover is a continuous process, dynamic fluctuations in receptor levels, mediated primarily by the ubiquitin-proteasome pathway, occur in response to changing cellular conditions. In the absence of ligand, ERα is sequestered within a stable chaperone protein complex consisting of heat shock protein 90 (Hsp90) and co-chaperones. However, the molecular mechanism(s) regulating ERα stability and turnover remain undefined. One potential mechanism involves CHIP, the carboxyl terminus of Hsc70-interacting protein, previously shown to target Hsp90 interacting proteins for ubiquitination and proteasomal degradation. In the present study, a role for CHIP in ERα protein degradation was investigated. In ER-negative HeLa cells transfected with ERα and CHIP, ERα proteasomal degradation increased, while ERα-mediated gene transcription decreased. In contrast, CHIP depletion by siRNA resulted in increased ERα accumulation and reporter gene transactivation. Transfection of mutant CHIP constructs demonstrated that both the U-box (containing ubiquitin ligase activity) and the tetratricopeptide repeat (TPR, essential for chaperone binding) domains within CHIP are required for CHIP-mediated ERα downregulation. In addition, coimmunoprecipitation assays demonstrated that ERα and CHIP associate through the CHIP TPR domain. In ERα-positive breast cancer MCF7 cells, CHIP overexpression resulted in decreased levels of endogenous ERα protein and attenuation of ERα-mediated gene expression. Furthermore, the ERα-CHIP interaction was stimulated by the Hsp90 inhibitor geldanamycin (GA), resulting in enhanced ERα degradation; this GA effect was further augmented by CHIP overexpression, but was abolished by CHIP depletion. Finally, ERα dissociation from CHIP by various ERα ligands,

4

including E2, OHT, and ICI, interrupted CHIP-mediated ERα degradation. These results

55 demonstrate a role for CHIP in both basal and GA-induced ERα degradation. Furthermore, based on our observations that CHIP promotes ERα degradation and attenuates receptor-mediated gene transcription, we suggest that CHIP, by modulating ERα stability, contributes to the regulation of functional receptor levels, and thus hormone responsiveness, in estrogen target cells.

60

INTRODUCTION

The primary mediators of 17β-estradiol (E2) action, the major female sex steroid hormone, are the estrogen receptors ERα and ERβ. These receptors function as ligand-activated transcription factors, regulating expression of genes coordinating most physiological and many

65   pathophysiological processes in estrogen target tissues (1). Tissue sensitivity, and the overall magnitude of response to E2 and other estrogens, is strongly influenced by a combination of factors, including cellular levels of ERα and its various coactivators and corepressors (2, 3).

To strictly control cellular responses, the cellular synthesis and turnover of the ERα protein dynamically fluctuates with changing cellular environments (4). For example, in the

70   absence of ligand, ERα is a short-lived protein (half-life of 4-5 hours) and undergoes constant degradation (5). In the presence of ligand, by contrast, the turnover rate of ERα can be increased or decreased, depending upon the ligand, thus modulating receptor protein levels. Turnover-inducing factors and conditions include the cognate ligand E2, pure antiestrogens (ICI 164,384, ICI 182,780, RU 58,668), Hsp90 inhibitors (geldanamycin and radicicol), ATP

75   depletion (oligomycin and hypoxia) and aryl hydrocarbon agonists; these all induce degradation and rapid downregulation of ERα levels (6-12). In contrast, the partial agonist/antagonist 4-hydoxytamoxifen (OHT), thyroid hormone, and protein kinase K activators (Forskolin, 8-bromo-cAMP) all block receptor degradation , subsequently increasing ERα protein levels (13-15).

Although both basal and ligand-induced ERα degradation are mediated by the ubiquitin-

80   proteasome pathway (12, 13, 16-21), regulation of this pathway, at the molecular level, remains unclear. Emerging evidence suggests that multiple ERα degradation pathways exist, and the engagement of one pathway over another depends on the nature of the stimulus (19, 21-23). For example, E2-induced receptor degradation is coupled with transcription and requires new protein

6

synthesis (17, 19, 22, 24); conversely, neither ERα transcriptional activity nor new protein

85   synthesis are needed for ICI 182,780-induced ERα degradation (19, 20, 22). In addition, various

stimuli induce distinct changes in the conformation and cellular compartmentalization of

ERα (22, 25-27), and these may be associated with receptor ubiquitination.

Like other members of the steroid receptor superfamily, unliganded ERα, by associating

with various Hsp90-based chaperone complexes, is maintained in a ligand-binding competent

90   conformation (28). Although these associations do not influence ERα ligand-binding affinity,

Hsp90 chaperone complexes appear to regulate ERα stability, as Hsp90 disruption induces rapid

ERα degradation through the ubiquitin proteasome pathway (9, 28, 29). For regulation of such

complexes, recent studies have identified the carboxyl terminus of Hsc70-interacting protein

(CHIP) as a ubiquitin ligase that directs chaperone substrates for ubiquitination and proteasomal

95   degradation (30, 31). CHIP interacts with Hsp/Hsc70 and Hsp90 through an amino-terminal

tetratricopeptide repeat (TPR) domain and catalyzes ubiquitin conjugation through a carboxyl-

terminal U-box domain (30). As recent observations demonstrate that CHIP targets a number of

Hsp70/90-associated proteins for ubiquitination and degradation, including the glucocorticoid

receptor, androgen receptor, Smad1/4, and ErbB2 (30-33), we investigated a regulatory role for

100   CHIP in ERα stability. Our results demonstrate that CHIP, likely through a chaperone

intermediate, associates with ERα and consequently facilitates both basal and geldanamycin-

induced receptor degradation in human cancer cells.

RESULTS

105   CHIP overexpression decreases and CHIP knockdown increases ERα protein levels

To investigate the effect of CHIP overexpression on steady state levels of ERα, ER-negative HeLa cells were cotransfected with constructs expressing CHIP (pcDNA-His6-CHIP) and ERα (pSG5-ERα). ERα protein levels were subsequently determined by immunoblot analysis. Overexpression of CHIP decreased ERα protein levels in a dose-dependent manner

110 (Fig. 1A). To control for transfection efficiency, the green fluorescence protein (GFP) was also included in transfection. No effect of CHIP on GFP expression level was observed (Fig. 1A), demonstrating that CHIP-induced downregulation of ERα was specific. Next, we examined whether CHIP-induced ERα downregulation could be inhibited by CHIP-specific siRNA. Compared to cells transfected with CHIP only, cotransfection of pBS/U6/CHIPi, a CHIP-siRNA

115 expression construct (33), dramatically decreased the level of exogenous CHIP (Fig. 1B, *upper panel*). However, pBS/U6/CHIPi had no effect on GFP level, confirming that the CHIP-siRNA specifically blocks CHIP expression (Fig 1B). The effect of CHIP-siRNA on CHIP-induced ERα downregulation was then examined. As shown in Fig. 1B (*lower panel*), cotransfection of CHIP-siRNA, in a dose-dependent fashion, attenuated ERα downregulation induced by

120 exogenous CHIP. Collectively, these results demonstrate that CHIP overexpression can downregulate ERα protein level in HeLa cells.

To examine a role for endogenous CHIP in regulation of ERα protein levels, HeLa cells, which are known to express CHIP (30), were cotransfected with pBS/U6/CHIPi and ERα. Expression of CHIP-siRNA decreased the level of endogenous CHIP by 60%, and

125 correspondingly increased ERα protein level by 1.6 fold (Fig. 1C), indicating that endogenous CHIP plays a role in controlling ERα level in HeLa cells.

CHIP down-regulates ERα levels through the ubiquitin proteasome pathway

To determine whether proteasome activity is required for CHIP-induced ERα
130   downregulation, HeLa cells were cotransfected with pcDNA-His6-CHIP and pSG5-ERα, treated

with the protease inhibitor MG132, and subjected to immunoblotting. As shown in Fig. 2A, 6-hr

treatment with MG132 completely blocked CHIP-induced downregulation of ERα. To examine

whether polyubiqutination is required for CHIP-induced ERα degradation, a mutant ubiquitin,

UbK0, with all lysines replaced by arginines (34), was utilized. Previously, we showed that the

135   UbK0 protein could efficiently block E2-induced ERα degradation (35). Expression of UbK0,

but not wild-type ubiquitin, restored ERα protein levels (Fig. 2B), demonstrating that CHIP

stimulates ERα degradation through the ubiquitin and proteasome pathway.

CHIP targets mature ERα for degradation

140   It has been proposed that CHIP functions as a general ubiquitin ligase, responsible for

ubiquitinating unfolded or misfolded proteins in a chaperone-dependent process (31). To

examine whether ERα downregulation by CHIP was due to the selective ubiquitination of

unfolded or misfolded receptor protein, we examined the effect of OHT, a selective estrogen

receptor modulator, on CHIP-mediated ERα degradation. It has been shown that OHT can

145   dissociate ERα from its chaperone complex and protect the receptor from both basal turnover

and degradation induced by Hsp90-binding agents (8, 13, 21). We reasoned that if CHIP

selectively targets immature or misfolded ERα (with no functional OHT-binding pocket), then,

in the presence of CHIP, OHT treatment should not restore ERα levels. On the other hand, if

CHIP targets mature ERα, OHT treatment should rescue the receptor protein from CHIP-induced

9

150   degradation. HeLa cells were thus cotransfected with pcDNA-His6-CHIP and pSG5-ERα and

treated with OHT for 6 h prior to lysate preparation. OHT treatment completely abolished

CHIP-induced ERα downregulation (Fig. 2A), but had no effect on protein levels of CHIP and

GFP, excluding the possibility that OHT treatment affects protein degradation in general. These

results demonstrate that CHIP induces degradation of correctly folded, ligand-binding competent

155   ERα.

Both the TPR and U-box domains are essential for CHIP-induced ERα downregulation

To examine whether the ubiquitin ligase activity and chaperone interaction domain are

required for CHIP-induced ERα degradation, two mutant CHIP constructs were utilized: 1)

160   CHIP(K30A), a TPR domain mutant unable to interact with Hsp/Hsc70 or Hsp90; and 2)

CHIP(H260Q), a U-box domain mutant unable to catalyze protein ubiquitin conjugation (36). In

contrast to wild-type CHIP, neither CHIP(K30A) nor CHIP(H260Q) overexpression decreased

ERα protein levels (Fig. 3A). These results establish that both the chaperone interaction and

ubiquitin ligase activity of CHIP are required for CHIP-targeted degradation of ERα protein.

165

The TPR domain of CHIP is required for the CHIP-ERα interaction

As CHIP appears to be linked to ERα degradation, we investigated whether CHIP

associates with the receptor. HeLa cells were cotransfected with ERα and CHIP, and

coimmunoprecipitation analysis performed using an ERα-specific antibody. The results revealed

170   a complex containing both CHIP and ERα (Fig. 3B). Because CHIP(K30A) exhibited no effect

on ERα turnover (Fig. 3A), we examined whether the TPR domain is required for the CHIP-

ERα interaction. In HeLa cells cotransfected with ERα and CHIP(K30A), the CHIP mutant was

not detected in the precipitated ERα complex (Fig. 3B), demonstrating a requirement for the TPR domain in the CHIP-ERα interaction. Because it is known that CHIP interacts with Hsp90 or Hsc/Hsp70 through the TPR domain (30), our results suggest that a chaperone intermediate is involved in CHIP-induced ERα degradation.

CHIP interacts with endogenous ERα, in breast cancer cells, to induce receptor ubiquitination and degradation

Having demonstrated a role for CHIP (possibly in association with chaperones) in degradation of exogenous ERα in HeLa cells, it was of interest to examine the effect of CHIP on stability and function of endogenous ERα in breast cancer cells. In human breast cancer MCF7 cells, overexpression of CHIP resulted in a dose-dependent ERα downregulation (Fig. 4A). Coimmunoprecipitation analysis of MCF7 cells transfected with pcDNA-His6-CHIP revealed both CHIP and ERα in the immunocomplexes precipitated by either an ERα-specific or anti-His6 antibody (Fig. 4B), suggesting that CHIP associates with endogenous ERα. In addition, both Hsc70 and Hsp90 were detected in the precipitated ERα complex (Fig. 4B). These results indicate that CHIP can associate with endogenous ERα-Hsp90/Hsc70 complexes to downregulate ERα level in breast cancer cells.

To determine whether CHIP promotes polyubiquitination of endogenous ERα, we examined the ubiquitination status of ERα in MCF7 cells transfected with hemagglutinin-tagged ubiquitin (HA-Ub), plus a vector control (pcDNA) or a CHIP-expressing construct. To block proteasomal degradation of polyubiquitinated proteins, transfected cells were treated with MG132 for 6 h prior to lysate preparation. An ERα-specific antibody was then used for

11

195   immunoprecipitation, and the presence of ubiquitinated ERα in the immunocomplex was

detected by immunoblotting with an HA antibody. To assess overall levels of protein

ubiquitination, whole cell lysates were immunoblotted using an HA antibody. The

polyubiquitinated ERα exhibited a typical high molecular weight smear on the blot membrane,

and overexpression of CHIP markedly increased smear intensity, suggesting elevated receptor

200   polyubiquitination (Fig. 4C, *left panel*). In contrast, CHIP had no effect on overall protein

ubiquitination (Fig. 4C, *right panel*).

A possible limitation of *in vivo* ubiquitination assays is that the immunocomplex may

contain multiple polyubquitinated species, not just the target protein of interest. In order to

corroborate the observation that CHIP promotes ERα ubiquitination, we examined the effect of

205   CHIP on ERα-ubiquitination in MCF7 cells transfected with UbK0. This mutant ubiquitin

competes with endogenous ubiquitin and terminates ubiquitin chains, resulting in the

accumulation of oligoubiquitin-ERα conjugates, which upon immunoblotting with ERα antibody

can be detected as mobility-shifted bands. In MCF7 cells transfected with wild-type ubiquitin,

overexpression of CHIP had no effect on the intensity of ERα-ubiquitination (Fig. 4D, *left panel*),

210   presumably due to the rapid degradation of polyubiquitinated ERα. However, in cells

transfected with UbK0, overexpression of CHIP remarkably increased the amount of

oligoubiquitinated ERα (Fig. 4D, *right panel*), confirming that overexpression of CHIP promotes

ERα ubiquitination. Together, these results suggest that CHIP, by facilitating receptor

ubiquitination, targets endogenous ERα for proteasome-mediated degradation.

215

Knockdown of endogenous CHIP by siRNA increases ERα level in MCF7 cells

The above experiments showed that overexpression of CHIP promotes ERα polyubiquitination and degradation in breast cancer cells. Conversely, we wanted to examine whether knockdown of endogenous CHIP protein by CHIP-siRNA could increase endogenous

220 ERα level. Transfection of MCF7 cells with pBS/U6/CHIPi decreased the level of endogenous CHIP by 60% (Fig. 4E, *upper panel*) and increased the level of ERα level by 1.5 fold (Fig. 4E, *lower panel*), indicating that endogenous CHIP plays a role in basal turnover of ERα in breast cancer cells.

225 **CHIP downregulates ERα-mediated gene expression**

Having established a role for CHIP in ERα ubiquitination and receptor turnover, we next examined the effect of CHIP on ERα-mediated gene transactivation. HeLa cells were transiently transfected with ERα and an estrogen responsive reporter (ERE-pS2-Luc), plus various CHIP (CHIP, H260Q, K30A, CHIP-siRNA) or control (pcDNA) constructs. Twenty-four hours after

230 transfection, cells were treated for 6 h with vehicle (DMSO) or E2 (10 nM) and luciferase activity then measured. In a parallel experiment, a constitutive reporter (SV40-Luc) was used to monitor transcription efficiency, as well as any general effects of the various CHIP constructs might have on luciferase expression. The ERE-pS2-Luc activities were then normalized to the corresponding SV40-Luc activities. Expression of wild type CHIP decreased ($P<0.05$) E2-

235 induced ERE-pS2-Luc expression, while the CHIP mutants had no effect on ERα-mediated gene transactivation (Fig. 5A). Conversely, depletion of endogenous CHIP by siRNA increased both basal and E2-induced ERE-pS2-Luc expression (($P<0.01$, Fig. 5B). Similarly, in MCF7 cells, overexpression of CHIP, but not U-box or TPR mutant, attenuated ERα-mediated reporter gene expression (Fig. 6A), while knockdown of endogenous CHIP by siRNA augmented ERα-

13

240 mediated reporter gene expression (Fig. 6B). To examine the effect of knocking down CHIP on

the expression of an endogenous ERα target gene, MCF7 cells were transfected with CHIP-

siRNA, and *pS2* mRNA levels were examined. As shown in Fig. 6C, both basal and E2-induced

expression of *pS2* mRNA were significantly increased. Together, these results demonstrate that

CHIP coordinately regulates ERα protein levels and ERα-mediated gene transactivation.

245

Geldanamycin induces ERα degradation through a CHIP-dependent mechanism

The Hsp90 inhibitor, geldanamycin (GA), binds to the amino-terminal ATP/ADP-binding

domain of Hsp90, "locking" this chaperone protein in its ADP-bound conformation (9, 29, 37).

CHIP has been reported to play a role in GA-induced degradation of ErbB2, a Hsp90 client

250 protein (36, 38), and recent studies have shown that GA stimulates ERα degradation through the

ubiquitin-proteasome pathway (9, 29, 37). Whether CHIP plays a role in GA-induced ERα

degradation has not been previously investigated. Thus, we examined the effects of CHIP

overexpression and depletion on GA-induced ERα degradation. In HeLa cells transfected with

ERα, GA treatment resulted in a time-dependent ERα downregulation (Fig. 7A); this effect was

255 enhanced by CHIP overexpression (Fig. 7A). Conversely, CHIP depletion by siRNA completely

abolished GA-induced ERα downregulation (Fig. 7A).

To investigate the effect of GA on the CHIP-ERα interaction, HeLa cells were

transfected with ERα and CHIP, and coimmunoprecipition was performed with an ERα-specific

antibody. The amount of CHIP in the precipitated ERα complex increased following a 1-hr GA

260 treatment (Fig. 7B), suggesting that GA promotes ERα degradation by recruiting CHIP to the

chaperone-ERα complex. Because CHIP can associate with ubiquitinated proteins through its

U-box domain (31), ERα ubiquitination may play a role in the GA-induced ERα-CHIP

14

interaction. We thus examined the interaction between ERα and CHIP in the presence of the

proteasome inhibitor MG132. We reasoned that if CHIP preferentially interacts with

265   ubiquitinated ERα, then MG132, by enhancing the accumulation of polyubiquitinated ERα,

would increase the ERα-CHIP interaction. However, MG132 treatment did not increase the

amount of CHIP precipitated with the ERα complex (Fig. 7B), suggesting that the GA-induced

ERα-CHIP interaction occurs prior to ERα polyubiquitination.

To establish a role for CHIP in GA-induced ERα degradation under physiologically

270   relevant conditions, the consequence of knocking down endogenous CHIP by siRNA on ERα

degradation was examined in MCF7 cells. GA induced rapid ERα downregulation in MCF7

cells transfected with a pcDNA control plasmid (Fig. 8A), consistent with previous reports (9,

29). However, expression of CHIP-siRNA significantly impaired GA-induced ERα

downregulation (Fig. 8A). In addition, we performed a coimmunoprecipitation analysis to

275   examine the effect of GA treatment on the association between endogenous CHIP and ERα. As

shown in Fig. 8B, GA treatment increased the amount of CHIP that coimmunoprecipitated with

ERα. Based on these results, we suggest that GA induces ERα degradation by enhancing the

recruitment of CHIP to ERα-chaperone complexes.

280   **Effects of ligand binding on geldanamycin-induced ERα degradation**

Ligand binding results in disassembly of the ERα-Hsp90 chaperone complex, due to

competition for overlapping binding sites and conformational changes within the ERα protein

(28). Since GA stimulated the CHIP-ERα interaction (Fig. 7B and 8B), we investigated whether

ligand binding, by interrupting the CHIP-ERα interaction, could interfere with GA-induced ERα

285   degradation. Towards this, ERα protein levels were examined in MCF7 cells: 1) exposed to E2,

ICI 182,780 (ICI) or GA alone; 2) pretreated with vehicle, E2, OHT or ICI for 30 min, followed

by a 6-h treatment with GA; and 3) pretreated with vehicle or GA for 30 min, followed by a 5.5-

hr treatment with E2, OHT or ICI. As expected, E2, ICI and GA treatment, but not OHT,

dramatically downregulated ERα levels in MCF7 cells (Fig. 9A, *upper panel*). Exposure to E2

290   or OHT, either prior to (Fig. 9A, *middle panel*) or shortly after (Fig. 9A, *lower panel*) GA

treatment, completely abolished GA-induced ERα degradation.   In contrast to what was

observed with E2 and OHT, ICI exposure, neither prior to (Fig. 9A, *middle panel*) nor shortly

after (Fig. 9A, *lower panel*) GA treatment, failed to protect ERα against degradation.

To   examine   the   effect   of   these   ligands   on   the   CHIP-ERα   interaction,

295   coimmunoprecipitation analysis was performed on MCF7 cells transfected with CHIP. Cells

were pretreated with GA for 30 min, followed by a 30-min treatment with E2, OHT, or ICI. GA

treatment alone increased the amount of CHIP detected in the precipitated ERα complex;

however, this amount was substantially reduced by treatment with E2, OHT, or ICI (Fig. 9B).

These results demonstrate that all three ligands can interfere with the interaction between CHIP

300   and ERα. Because these ligands have dramatically different effects on ERα stability, our results

indicate that after dissociation from the Hsp90 chaperone complex, distinct downstream

pathways exist for ERα degradation. Because E2 alone can induce ERα degradation through a

transcription coupled mechanism (17, 19, 22, 24), it was somewhat unexpected to observe that

ERα was stable during the combined treatment of GA and E2 (Fig. 9A). One explanation is that

305   Hsp90 activity (inhibited by GA) is required for transcription-coupled ERα degradation. The

OHT-ERα complex lacks transcriptional activity in MCF7 cells and thus is not a substrate for the

transcription-coupled degradation pathway. Consequently, the ability of OHT to block GA-

induced ERα degradation is likely due to disruption of the CHIP-ERα interaction (Fig. 9B). ICI

also interrupts the GA-induced CHIP-ERα interaction (Fig. 9B) but fails to stabilize ERα (Fig.

310   9A), suggesting that the ERα-ICI complex is targeted for degradation through a CHIP-

independent, GA-insensitive pathway.

Effect of CHIP and geldanamycin on ERα cellular localization

CHIP and Hsp90 are located primarily in the cytoplasm (30), while ERα is primarily a

315   nuclear-localized protein (39). To determine whether CHIP overexpression, or GA treatment,

could affect the cellular distribution of ERα, HeLa cells were transfected with a GFP-ERα

fusion protein (40) and the cellular distribution of green fluorescence was examined. In control

cells, fluorescence was restricted to the nuclei (Fig. 10A, *top left panel*). CHIP coexpression or

GA treatment did not affect the nuclear localization of GFP-ERα (Fig. 10A). In contrast, ICI

320   treatment, either alone or in the presence of transfected CHIP, resulted in the appearance of

green fluorescence in the cytoplasm (Fig. 10A, *bottom two panels*). This observation is

consistent with a previous study by Dauvois *et al.* showing that ICI induces cytoplasmic

retention of ERα (7). In addition, in HeLa cells transfected with GFP-ERα only, treatment with

GA resulted in the appearance of GFP foci in the nuclei of approximately 20% of transfected

325   cells (Fig. 10A, *left middle panel*). These GFP foci were not observed in GA-treated cells

cotransfected with CHIP (Fig. 10A, *right middle panel*). While the identity of the GFP foci is

unknown, one possibility is that these represent aggregated GFP-ERα, resulting from the

combined effect of Hsp90 inhibition and high expression levels of GFP-ERα. CHIP

overexpression may promote both basal and GA-induced ERα degradation, preventing GFP-

330   ERα aggregate formation. Consistent with this interpretation, we found that expression of CHIP

17

decreased the number of GFP-ERα-expressing cells (Fig. 10B). Based on our results, and a recent finding that a small fraction of nuclear-localized CHIP can promote nuclear protein degradation (41), we suggest that CHIP-mediated ERα degradation occurs within the nucleus.

335   DISCUSSION

The cellular level of ERα determines both estrogen sensitivity and responsiveness (2, 35, 42). Steady state levels of ERα protein are tightly regulated through a rapid balance between receptor synthesis and turnover, according to changing cellular conditions (4). Although it has been well documented that ERα degradation is primarily mediated by the ubiquitin proteasome

340   pathway, the molecular mechanism(s) by which cells regulate ERα stability are largely unknown. Here we report that the Hsc70/Hsp90-interacting protein CHIP plays a key role in both basal and Hsp90 inhibitor-induced ERα turnover. Furthermore, CHIP-induced receptor degradation occurs through the ubiquitin proteasome pathway. Overexpression of CHIP promotes ERα degradation, accompanied by a decrease in ERα-mediated gene transactivation.

345   Conversely, inhibition of CHIP by siRNA increases ERα levels and upregulates ERα-mediated gene transactivation. Thus, this is the first report that CHIP, by modulating the cellular concentration of ERα, plays a role in regulating estrogen action.

During the preparation of this report, Tateishi and colleagues reported a similar finding, that CHIP plays a role in basal ERα turnover (43). Our findings agree with several conclusions

350   from that study, including: 1) CHIP, through its TPR domain, associates with ERα-chaperone complexes; 2) CHIP promotes, through its TPR and U-box domains, both polyubiquitination and proteasomal degradation of unliganded ERα; 3) CHIP-mediated ERα degradation occurs in the

18

nucleus; and 4) ligand binding blocks CHIP-mediated ERα degradation by disrupting CHIP-ERα interaction. Here, we further extend the study of Tateishi *et al.* (43) in two significant

355   aspects: 1) CHIP is required for Hsp90 inhibitor-induced ERα degradation; and 2) CHIP targets "functional" ERα (correctly folded, ligand-binding competent receptor protein) for degradation (43).

Several lines of evidence from our study support the conclusion that CHIP targets functional ERα for degradation. First, OHT treatment completely blocked CHIP-induced ERα

360   degradation, suggesting that ERα reaches a correctly folded conformation, competent for ligand binding, prior to CHIP-directed degradation. Secondly, CHIP overexpression downregulated ERα levels and decreased ERα-mediated gene expression, while CHIP depletion by siRNA upregulated ERα levels and increased ERα-mediated gene transcription. This coordinate regulation of ERα levels and activity suggests that CHIP targets functional ERα for degradation.

365   Thirdly, CHIP plays a role in GA-induced ERα degradation by primarily targeting Hsp90-associated, transcriptionally competent ERα (29). Although originally believed to function as a general ubiquitin ligase, responsible for ubiquitinating unfolded or misfolded proteins in a chaperone-dependent process (31), more recent studies have demonstrated that CHIP also targets mature Hsp90 client proteins for degradation (33, 36).

370   Tateishi *et al.* (44) observed that CHIP overexpression increased ERα transcriptional activity. Although this was not observed in our study, the use of different estrogen-response element (ERE) and control reporter constructs for the functional analyses of ERα could account for this discrepancy. In the present study, an estrogen-responsive reporter construct (ERE-pS2-Luc), possessing two ERE copies within the pS2 promoter (44), was used. Our previous study

375   demonstrated a close correlation between ERE-pS2-Luc expression and cellular concentration of

19

ERα (35). In the present study, we also utilized a constitutively active construct, SV40-Luc, to monitor and normalize the effects of both CHIP and CHIP-siRNA on transfection efficiency and luciferase expression. In the study by Tateishi *el al.,* pRSVβGal was used as an internal control (44). When we used a similar construct, CMVβGal, we found that overexpression of either wild-type CHIP or TPR mutant (K30A), but not U-box mutant (H260Q), dramatically decreased CMVβGal expression in a dose-dependent manner (data not shown). Based on these observations, we suggest that βGal is not a suitable control reporter for studying the effect of CHIP on gene transcription.

Our results, with data from Tateishi *et al.* (44), suggest a role for the Hsp90 chaperone complex in the regulation of cellular ERα levels. A summary of distinct ERα degradation pathways is depicted in Fig. 11. Nascent ERα is translocated into nucleus, and by associating with Hsp90, receptor protein is maintained in a ligand-binding competent conformation, ready for subsequent activation (28). In the absence of ligand or other activation signals, CHIP constantly targets chaperone-associated ERα for degradation, thereby limiting cellular concentrations of receptor protein. Ligand binding disassembles the ERα-Hsp90 complex and thus protects ERα from CHIP-mediated degradation. However, depending on the ligand, ERα stability can vary considerably, suggesting that different downstream destructive pathways exist. Furthermore, the ERα-ligand interaction could play a definitive role in pathway utilization. For example, when activated by E2, ERα is degraded through a transcription-coupled mechanism (17, 19, 22, 24). Pretreatment with GA, however, abolished E2-induced ERα degradation (Fig. 9A), suggesting that Hsp90 activity is required for transcription-coupled ERα degradation. In support of this possibility, the Hsp90-p23 complex has been shown to play a role in disassembling the nuclear receptor transcriptional complex from chromatin, a process believed to

20

be a prerequisite for degradation of activated transcription factors (45-47). Conversely, through

400 an unknown mechanism, the nuclear ERα-ICI complex is immobilized to the nuclear matrix and

undoes rapid degradation, in association with cytoplasmic retention of aggregated nascent

ERα (7, 8, 22, 27, 40, 48). While it not clear how intracellular localization influences receptor

degradation, the unique distribution pattern of ERα after treatment with ICI-182,780, together

with the fact that ICI-induced receptor degradation is *independent* of ERα transcription activity,

405 support the possibility that the pure antiestrogen and E2 utilize distinct degradation pathways for

ERα. Taken together with our previous observation that an intact NEDD8 conjugation pathway

is essential for ICI-induced ERα degradation in breast cancer cells (49), we suggest that

destruction of the ICI-liganded receptor requires a cullin-based ubiquitin ligase.

Abnormal expression of ERα has long been associated with both the initiation and

410 progression of breast cancer (50). An increase in the number of ERα-positive cells, as well as

increased individual cell ERα content, have frequently been detected in malignant breast tumors

(42). Furthermore, increased ERα content has been shown to augment the magnitude of

estrogen-stimulated gene expression, providing a growth advantage to breast cancer cells (2, 35,

49, 51). A recent study demonstrated a correlation between the loss of ERK7, a regulator of

415 estrogen-induced ERα degradation, and breast cancer progression (52). Collectively, these

observations indicate that alterations in ERα degradation pathways may contribute to

deregulation of ERα, perhaps leading to enhanced estrogen action in breast tumors. Based on our

results, the chaperone/CHIP pathway, by regulating ERα levels, likely contributes to the

development/progression of that disease; and such a possible role merits further examination.

MATERIALS AND METHODS

420

Materials

The following antibodies and reagents were used in this study: anti-ERα (HC20) and anti-β-tubulin (SC9104) (Santa Cruz Biotechnology, Santa Cruz, CA); anti-HA tag (3F10; Roche Molecular Biochemicals, Indianapolis, IN); anti-ERα (Ab-10) and anti-GFP (GFP01)

425 (NeoMarkers, Inc., Fremont, CA); anti-GAPDH (Chemicon International, Inc., Temecula, CA); anti-CHIP (PA1-015, Affinity Bioreagents, Golden, CO); anti-Hsp90 (SPA-830) and anti-Hsc70 (SPA-816) (Stressgene, Victoria, BC, Canada); anti-His6 (8906-1, BD Biosciences, Palo, Alto, CA); protein G-agarose beads (Oncogene Research Products, San Diego, CA); horseradish peroxidase-conjugated second antibodies and SuperSignal West Pico Chemiluminescent

430 Substrate (Pierce, Rockford, IL); protein assay kit (Bio-Rad laboratories Inc., Hercules, CA); protease inhibitor cocktail set III (Calbiochem-Novabiochem Corporation, San Diego, CA); LipofectAMINE Plus Reagent (Life Technologies, Inc., Logan, UT); FuGENE (Roche Molecular Biochemicals, Indianapolis, IN); 17β-estradiol, 4-hydroxytamoxifen, geldanamycin and MG132 (Sigma Chemical Co., St. Louis, MO); ICI 182,780 (Tocris Cookson Ltd.,

435 Ellisville, MO); Passive lysis buffer and luciferase assay system (Promega Corp., Medison, WI); fetal bovine serum (FBS) and dextran-coated charcoal-stripped FBS (csFBS) (Hyclone laboratories, Inc., Logan, Utah); cell culture supplementary reagents (Life Technologies, Inc.; Rockville, MD).

440 **Plasmid Construction**

The construction of pSG5-ERα(HEGO), ERE2-pS2-Luc, SV40-Luc, pcDNA-HA-Ub, pCS2-UbK0 and CMV-GFP have all been described previously (35). The pcDNA-His6-CHIP,

22

pcDNA-His6-CHIP(K30A), and pcDNA-CHIP(H260Q) constructs were kindly provided by Dr.

Neckers and Cam Patterson (36), the pBS/U6/CHIPi construct by Dr. Chang (33), and the GFP-

445   ERα construct by Dr. Stenoien (40).

Cell Lines and Transient Transfection

The human cervical carcinoma cell line HeLa and the breast cancer cell line MCF-7 were

purchased from ATCC (Manassas, VA). HeLa cells were maintained in minimum essential

450   medium (MEM) with 2 mM L-glutamine, 1.5 g/L sodium bicarbonate, 0.1 mM non-essential

amino acids, 1.0 mM sodium pyruvate, 50 units/ml penicillin, 50 µg/ml streptomycin, and 10%

FBS. MCF7 cells were maintained in the same medium, with the addition of 6 ng/ml insulin.

Prior to experiments, cells were cultured in hormone-free medium (phenol red free MEM with

3% dextran-coated charcoal-stripped FBS (csFBS)) for 3 days. For transfection, cells (80%

455   confluence) were transfected with an equal amount of total plasmid DNA (adjusted with the

corresponding empty vectors) by using LipofectAMINE Plus Reagent or FuGENE according to

the manufacturer's guidelines.

Immunoblotting, Immunoprecipitation and Luciferase Assay

460   For immunoblot analysis, whole cell extracts were prepared by suspending cells ($\sim$2 x 10^6) in 0.1

ml SDS lysis buffer (62 mM Tris, pH 6.8, 2% SDS, 10% glycerol, and protease inhibitor cocktail

III). After 15 min incubation on ice, extracts were sonicated (3 x 20 sec), insoluble material

removed by centrifugation (15 min at 12,000 x g), and supernatant protein concentration

determined using a BioRad protein assay kit. Five percent β-mercaptoethanol was added to the

465   protein extracts before heating at 90 ^{0}C for 5 min. Protein extracts (50 µg per lane) were

23

fractionated by SDS-PAGE, transferred to polyvinylidene difluoride (PVDF) membranes, and probed with antibodies. Primary antibody was detected by horseradish peroxidase-conjugated second antibody and visualized using an enhanced SuperSignal West Pico Chemiluminescent Substrate. The band density of exposed films was evaluated with ImageJ software

470 (http://rsb.info.nih.gov/ij/). Immunoprecipitation was performed as described previously (49). For luciferase assays, cell lysates were prepared with passive lysis buffer and luciferase activity determined using the Luciferase Assay System.

CHIP siRNA construct

475 The pBS/U6/CHIPi construct was kindly provided by Dr. Zhijie Chang (33). The siRNA expressed by the pBS/U6/CHIPi construct starts with GGG (position 233 to 251 bp relative to the ATG start site in the CHIP cDNA).

Quantitative Real Time PCR (Q-PCR)

480 Total RNA was prepared by a RNAeasy Mini Kit (Qiagen, Valencia, CA), according to the manufacturer's protocol. RNA (2 μg) was reverse-transcribed in a total volume of 40 μl containing 400 units M-MLV (New England Biolabs, Beverly, MA), 400 ng random hexamers (Promega), 80 units RNase Inhibitor and 1 mM dNTPs. The resulting cDNA was used in subsequent Q-PCR reactions, performed in 1x iQ SYBR Green Supermix (Bio-Rad) with 5 pmol

485 forward and reverse primers as previously described (35).

24

REFERENCE

1. Barkhem T, Nilsson S, Gustafsson JA 2004 Molecular mechanisms, physiological consequences and pharmacological implications of estrogen receptor action. Am J Pharmacogenomics 4:19-28

490 2. Webb P, Lopez GN, Greene GL, Baxter JD, Kushner PJ 1992 The limits of the cellular capacity to mediate an estrogen response. Mol Endocrinol 6:157-67

3. Klinge CM 2000 Estrogen receptor interaction with co-activators and co-repressors. Steroids 65:227-51.

4. Reid G, Denger S, Kos M, Gannon F 2002 Human estrogen receptor-alpha: regulation by

495 synthesis, modification and degradation. Cell Mol Life Sci 59:821-31

5. Eckert RL, Mullick A, Rorke EA, Katzenellenbogen BS 1984 Estrogen receptor synthesis and turnover in MCF-7 breast cancer cells measured by a density shift technique. Endocrinology 114:629-37

6. Dauvois S, Danielian PS, White R, Parker MG 1992 Antiestrogen ICI 164,384 reduces

500 cellular estrogen receptor content by increasing its turnover. Proc Natl Acad Sci U S A 89:4037-41

7. Dauvois S, White R, Parker MG 1993 The antiestrogen ICI 182780 disrupts estrogen receptor nucleocytoplasmic shuttling. J Cell Sci 106:1377-88

8. Devin-Leclerc J, Meng X, Delahaye F, Leclerc P, Baulieu EE, Catelli MG 1998

505 Interaction and dissociation by ligands of estrogen receptor and Hsp90: the antiestrogen RU 58668 induces a protein synthesis-dependent clustering of the receptor in the cytoplasm. Mol Endocrinol 12:842-54

9.   Bagatell R, Khan O, Paine-Murrieta G, Taylor CW, Akinaga S, Whitesell L 2001 Destabilization of steroid receptors by heat shock protein 90-binding drugs: a ligand-independent approach to hormonal therapy of breast cancer. Clin Cancer Res 7:2076-84

10.   Stoner M, Saville B, Wormke M, Dean D, Burghardt R, Safe S 2002 Hypoxia induces proteasome-dependent degradation of estrogen receptor alpha in ZR-75 breast cancer cells. Mol Endocrinol 16:2231-42

11.   Wormke M, Stoner M, Saville B, Safe S 2000 Crosstalk between estrogen receptor alpha and the aryl hydrocarbon receptor in breast cancer cells involves unidirectional activation of proteasomes. FEBS Lett 478:109-12

12.   Alarid ET, Bakopoulos N, Solodin N 1999 Proteasome-mediated proteolysis of estrogen receptor: a novel component in autologous down-regulation. Mol Endocrinol 13:1522-34

13.   Laios I, Journe F, Laurent G, Nonclercq D, Toillon RA, Seo HS, Leclercq G 2003 Mechanisms governing the accumulation of estrogen receptor alpha in MCF-7 breast cancer cells treated with hydroxytamoxifen and related antiestrogens. J Steroid Biochem Mol Biol 87:207-21

14.   Alarid ET, Preisler-Mashek MT, Solodin NM 2003 Thyroid Hormone Is an Inhibitor of Estrogen-Induced Degradation of Estrogen Receptor-alpha Protein: Estrogen-Dependent Proteolysis Is Not Essential for Receptor Transactivation Function in the Pituitary. Endocrinology 144:3469-76

15.   Tsai HW, Katzenellenbogen JA, Katzenellenbogen BS, Shupnik MA 2004 Protein kinase A activation of estrogen receptor alpha transcription does not require proteasome activity and protects the receptor from ligand-mediated degradation. Endocrinology 145:2730-8

530   16.   El Khissiin A, Leclercq G 1999 Implication of proteasome in estrogen receptor degradation. FEBS Lett 448:160-6.

17.   Lonard DM, Nawaz Z, Smith CL, O'Malley BW 2000 The 26S proteasome is required for estrogen receptor-alpha and coactivator turnover and for efficient estrogen receptor-alpha transactivation. Mol Cell 5:939-48

535   18.   Nawaz Z, Lonard DM, Dennis AP, Smith CL, O'Malley BW 1999 Proteasome-dependent degradation of the human estrogen receptor. Proc Natl Acad Sci U S A 96:1858-62

19.   Wijayaratne AL, McDonnell DP 2001 The human estrogen receptor-alpha is a ubiquitinated protein whose stability is affected differentially by agonists, antagonists, and selective estrogen receptor modulators. J Biol Chem 276:35684-92

540   20.   Reid G, Hubner MR, Metivier R, Brand H, Denger S, Manu D, Beaudouin J, Ellenberg J, Gannon F 2003 Cyclic, Proteasome-Mediated Turnover of Unliganded and Liganded ERalpha on Responsive Promoters Is an Integral Feature of Estrogen Signaling. Mol Cell 11:695-707

21.   Nonclercq D, Journe F, Body JJ, Leclercq G, Laurent G 2004 Ligand-independent and 545   agonist-mediated degradation of estrogen receptor-alpha in breast carcinoma cells: evidence for distinct degradative pathways. Mol Cell Endocrinol 227:53-65

22.   Stenoien DL, Patel K, Mancini MG, Dutertre M, Smith CL, O'Malley BW, Mancini MA 2001 FRAP reveals that mobility of oestrogen receptor-alpha is ligand- and proteasome-dependent. Nat Cell Biol 3:15-23.

550   23.   Marsaud V, Gougelet A, Maillard S, Renoir JM 2003 Various phosphorylation pathways, depending on agonist and antagonist binding to endogenous estrogen receptor alpha

27

(ERalpha), differentially affect ERalpha extractability, proteasome-mediated stability, and transcriptional activity in human breast cancer cells. Mol Endocrinol 17:2013-27

24.   Shao W, Keeton EK, McDonnell DP, Brown M 2004 Coactivator AIB1 links estrogen

555   receptor transcriptional activity and stability. Proc Natl Acad Sci U S A 101:11599-604

25.   Brzozowski AM, Pike AC, Dauter Z, Hubbard RE, Bonn T, Engstrom O, Ohman L, Greene GL, Gustafsson JA, Carlquist M 1997 Molecular basis of agonism and antagonism in the oestrogen receptor. Nature 389:753-8

26.   Wijayaratne AL, Nagel SC, Paige LA, Christensen DJ, Norris JD, Fowlkes DM,

560   McDonnell DP 1999 Comparative analyses of mechanistic differences among antiestrogens. Endocrinology 140:5828-40

27.   Htun H, Holth LT, Walker D, Davie JR, Hager GL 1999 Direct visualization of the human estrogen receptor alpha reveals a role for ligand in the nuclear distribution of the receptor. Mol Biol Cell 10:471-86

565   28.   Pratt WB, Toft DO 1997 Steroid receptor interactions with heat shock protein and immunophilin chaperones. Endocr Rev 18:306-60

29.   Lee MO, Kim EO, Kwon HJ, Kim YM, Kang HJ, Kang H, Lee JE 2002 Radicicol represses the transcriptional function of the estrogen receptor by suppressing the stabilization of the receptor by heat shock protein 90. Mol Cell Endocrinol 188:47-54

570   30.   Ballinger CA, Connell P, Wu Y, Hu Z, Thompson LJ, Yin LY, Patterson C 1999 Identification of CHIP, a novel tetratricopeptide repeat-containing protein that interacts with heat shock proteins and negatively regulates chaperone functions. Mol Cell Biol 19:4535-45

31.   Connell P, Ballinger CA, Jiang J, Wu Y, Thompson LJ, Hohfeld J, Patterson C 2001 The

575   co-chaperone CHIP regulates protein triage decisions mediated by heat-shock proteins.

        Nat Cell Biol 3:93-6

32.   He B, Bai S, Hnat AT, Kalman RI, Minges JT, Patterson C, Wilson EM 2004 An

        androgen receptor NH2-terminal conserved motif interacts with the COOH terminus of

        the Hsp70-interacting protein (CHIP). J Biol Chem 279:30643-53

580 33. Li L, Xin H, Xu X, Huang M, Zhang X, Chen Y, Zhang S, Fu XY, Chang Z 2004 CHIP

        mediates degradation of Smad proteins and potentially regulates Smad-induced

        transcription. Mol Cell Biol 24:856-64

34.   Bloom J, Amador V, Bartolini F, DeMartino G, Pagano M 2003 Proteasome-mediated

        degradation of p21 via N-terminal ubiquitinylation. Cell 115:71-82

585 35. Fan M, Nakshatri H, Nephew KP 2004 Inhibiting proteasomal proteolysis sustains

        estrogen receptor-alpha activation. Mol Endocrinol 18:2603-15

36.   Xu W, Marcu M, Yuan X, Mimnaugh E, Patterson C, Neckers L 2002 Chaperone-

        dependent E3 ubiquitin ligase CHIP mediates a degradative pathway for c-ErbB2/Neu.

        Proc Natl Acad Sci U S A 99:12847-52

590 37. Grenert JP, Sullivan WP, Fadden P, Haystead TA, Clark J, Mimnaugh E, Krutzsch H,

        Ochel HJ, Schulte TW, Sausville E, Neckers LM, Toft DO 1997 The amino-terminal

        domain of heat shock protein 90 (hsp90) that binds geldanamycin is an ATP/ADP switch

        domain that regulates hsp90 conformation. J Biol Chem 272:23843-50

38.   Zhou P, Fernandes N, Dodge IL, Reddi AL, Rao N, Safran H, DiPetrillo TA, Wazer DE,

595   Band V, Band H 2003 ErbB2 degradation mediated by the co-chaperone protein CHIP. J

        Biol Chem 278:13829-37

39. King WJ, Greene GL 1984 Monoclonal antibodies localize oestrogen receptor in the nuclei of target cells. Nature 307:745-7

40. Stenoien DL, Mancini MG, Patel K, Allegretto EA, Smith CL, Mancini MA 2000 Subnuclear trafficking of estrogen receptor-alpha and steroid receptor coactivator-1. Mol Endocrinol 14:518-34

41. Huang Z, Nie L, Xu M, Sun XH 2004 Notch-induced E2A degradation requires CHIP and Hsc70 as novel facilitators of ubiquitination. Mol Cell Biol 24:8951-62

42. Sommer S, Fuqua SA 2001 Estrogen receptor and breast cancer. Semin Cancer Biol 11:339-52

43. Tateishi Y, Kawabe Y, Chiba T, Murata S, Ichikawa K, Murayama A, Tanaka K, Baba T, Kato S, Yanagisawa J 2004 Ligand-dependent switching of ubiquitin-proteasome pathways for estrogen receptor. Embo J 23:4813-23

44. Fan M, Long X, Bailey JA, Reed CA, Osborne E, Gize EA, Kirk EA, Bigsby RM, Nephew KP 2002 The activating enzyme of NEDD8 inhibits steroid receptor function. Mol Endocrinol 16:315-30

45. Freeman BC, Yamamoto KR 2002 Disassembly of transcriptional regulatory complexes by molecular chaperones. Science 296:2232-5

46. Wochnik GM, Young JC, Schmidt U, Holsboer F, Hartl FU, Rein T 2004 Inhibition of GR-mediated transcription by p23 requires interaction with Hsp90. FEBS Lett 560:35-8

47. Morimoto RI 2002 Dynamic remodeling of transcription complexes by molecular chaperones. Cell 110:281-4

48. Pink JJ, Jordan VC 1996 Models of estrogen receptor regulation by estrogens and antiestrogens in breast cancer cell lines. Cancer Res 56:2321-30.

620   49.   Fan M, Bigsby RM, Nephew KP 2003 The NEDD8 pathway is required for proteasome-mediated degradation of human estrogen receptor (ER)-alpha and essential for the antiproliferative activity of ICI 182,780 in ERalpha-positive breast cancer cells. Mol Endocrinol 17:356-65

50.   Anderson E 2002 The role of oestrogen and progesterone receptors in human mammary
625   development and tumorigenesis. Breast Cancer Res 4:197-201

51.   Fowler AM, Solodin N, Preisler-Mashek MT, Zhang P, Lee AV, Alarid ET 2004 Increases in estrogen receptor-alpha concentration in breast cancer cells promote serine 118/104/106-independent AF-1 transactivation and growth in the absence of estrogen. Faseb J 18:81-93

630   52.   Henrich LM, Smith JA, Kitt D, Errington TM, Nguyen B, Traish AM, Lannigan DA 2003 Extracellular signal-regulated kinase 7, a regulator of hormone-dependent estrogen receptor destruction. Mol Cell Biol 23:5979-88

FIGURE LEGENDS

635   **Fig. 1.** CHIP overexpression decreases and CHIP knockdown increases ERα protein levels.

A. Overexpression of CHIP downregulates ERα protein levels. HeLa cells were transfected with

250 ng pSG5-ERα, 100 ng CMV-GFP, and various amounts (0, 50, 100 and 250 ng) of pcDNA-

his6-CHIP. *B. Expression of CHIP-siRNA attenuates CHIP-induced ERα downregulation.* In

the upper panel, HeLa cells were transfected with 250 ng pcDNA-his6-CHIP, with or without

640   250 ng pBS/U6/CHIPi, as indicated. In the lower panel, HeLa cells were transfected with 250 ng

pSG5-ERα, 250 ng pcDNA-his6-CHIP, and various doses (150, 300, 500, and 1000 ng) of

pBS/U6/CHIPi. *C. Knockdown of endogenous CHIP increases ERα level.* HeLa cells were

transfected with 250 ng pSG5-ERα and either 250 ng pcDNA-his6-CHIP or 250 ng

pBS/U6/CHIPi, as indicated. For all experiments, 3 x 10^5 HeLa cells were plated in 60-mm

645   dishes, cultured in hormone-free medium for 3 days, and then transfected with LipofectAMINE

Plus Reagent. Cell lysates were prepared 24 hr after transfection. Protein levels were

determined by immunoblotting with specific antibodies. Exogenous His6-CHIP and endogenous

CHIP were detected by anti-His6 and anti-CHIP, respectively. GFP and GAPDH were used as

transfection control and SDS-PAGE loading controls, respectively. Representative results of two

650   independent experiments, each performed in duplicate, are shown.

Fig. 2. The proteasome inhibitor MG132, partial ERα-antagonist OHT, and ubiquitin mutant

UbK0, all block CHIP-induced ERα degradation.

655   *A. The proteasome inhibitor MG132 and the partial ERα antagonist OHT block CHIP-induced*

ERα downregulation. HeLa cells were transfected with 250 ng pSG5-ERα and 100 ng CMV-

32

GFP, along with 250 ng pcDNA (vector control) or pcDNA-His6-CHIP, then treated with

DMSO (vehicle), 10 μM MG312 or 1 μM OHT for 6 hr prior to immunoblot analysis. Protein

levels of ERα, CHIP and GFP were determined by immunoblotting with anti-ERα, anti-His6 and

660   anti-GFP, respectively. GFP was used as a control for transfection efficiency and SDS-PAGE

loading. *B. Expression of the ubiquitin mutant UbK0 blocks CHIP-induced ERα*

downregulation. HeLa cells were transfected with 250 ng pSG5-ERα, with or without 250 ng

pcDNA-His6-CHIP, pcDNA-Ub or pCS2-UbK0, as indicated. ERα protein levels were

determined by immunoblotting with anti-ERα. GAPDH was used as a loading control for SDS-

665   PAGE. For all experiments, 3×10^5 HeLa cells were plated in 60-mm dishes, cultured in

hormone-free medium for 3 days, and then transfected with LipofectAMINE Plus Reagent. Cell

lysates were prepared 24 hr after transfection. The band density of exposed films was evaluated

with ImageJ software. Relative ERα levels were presented as the mean ± SE of three

independent experiments, each performed in duplicate.

670

Fig. 3. Both the TPR and U-box domains are required for CHIP-induced ERα downregulation.

A. Both the TRP and U-box domains are required for CHIP to downregulate ERα. HeLa cells

were transfected with 250 ng pSG5-ERα, 100 ng CMV-GFP, along with 250 pcDNA (control)

or various CHIP constructs as indicated. ERα and GFP protein levels were determined by

675   immunoblotting with anti-ERα and anti-GFP, respectively. GFP was used as control for

transfection efficiency and SDS-PAGE loading. *B. The TRP domain is required for CHIP-ERα*

interaction. HeLa cells were transfected with 250 ng pSG5-ERα, along with 250 ng pcDNA-

His6-CHIP or pcDNA-His6-CHIP(K30A). ERα protein in cell lysates was precipitated with

anti-ERα. The presence of CHIP in the precipitated ERα complex was determined by

680   immunoblotting with anti-His6. The same blot was re-probed with anti-ERα to assess the

amount of ERα in the precipitated immunocomplex. The expression levels of CHIP or

CHIP(K30A) in whole cell lysates was determined by immunoblotting with anti-His6 (lower

panel). For all experiments, HeLa cells were plated in 60-mm dishes at a density of $3x10^5$

cells/dish, cultured in hormone-free medium for 3 days, and then transfected with

685   LipofectAMINE Plus Reagent. Cell lysates were prepared 24 hr after transfection.

Representative results of two independent experiments, each performed in duplicate, are shown.

Fig. 4. CHIP interacts with endogenous ERα and induces ERα ubiquitination and degradation in

breast cancer MCF7 cells.

690   *A. Overexpression of CHIP downregulates endogenous ERα levels in MCF7 cells.* MCF7 cells

were plated in 100-mm dishes at a density of $1x10^6$ cells/dish, cultured in hormone-free medium

for 3 days, and transfected with various amounts (0, 5 or 10 μg) of pcDNA-His6-CHIP using

FuGENE. Twenty four hours after transfection, whole cell lysates were prepared, and protein

levels of ERα and CHIP determined by immunoblotting with anti-ERα and anti-His6,

695   respectively. GAPDH was used as an SDS-PAGE loading control. *B. CHIP associates with

ERα-Hsp complex in MCF7 cells.* MCF7 cells were transfected as in *A* and subjected to

coimmunoprecipitation analysis. ERα and CHIP were precipitated with anti-ERα and anti-His6,

respectively. The presence of CHIP, Hsc70, Hsp90 or ERα in the precipitated complexes was

determined by immunoblotting with anti-His6, anti-Hsc70, anti-Hsp90, or anti-ERα,

700   respectively. *C. Expression of CHIP enhances endogenous ERα polyubiquitination in MCF7*

cells. MCF7 cells were plated in 60-mm dishes at a density of 5×10^5 cells/dish cultured in hormone-free medium for 3 days, and transfected with 250 ng pcDNA-HA-Ub and 250 ng pcDNA or pcDNA-His6-CHIP. Twenty four hours after transfection, whole cell lysates were prepared and ERα protein was precipitated with anti-ERα. The presence of ubiquitin-conjugated

705 ERα in the immunocomplex was detected by immunoblotting with anti-HA (upper panel). The same membrane was reprobed with anti-ERα to assess the amount of precipitated ERα (middle panel). Whole cell lysates were separated by SDS-PAGE and probed with HA antibody to determine the amount of total ubiquitinated proteins (lower panel). *D. CHIP increases ERα ubiquitination in MCF7 cells expressing UbK0.* MCF7 cells were plated as in (*C*) and

710 transfected with 500 ng pcDNA-HA-Ub or 500 ng pCS2-UbK0, along with 250 ng pcDNA or pcDNA-His6-CHIP, as indicated. Twenty four hours after transfection, whole cell lysates were prepared and ERα protein was detected by immunoblotting with anti-ERα. *E. Knockdown of endogenous CHIP increases ERα level.* MCF7 cells were plated as in (*C*) and transfected with 2 μg vector or pBS/U6/CHIPi using FuGENE. Forty eight hours after transfection, whole cell

715 lysates were prepared, and protein levels of CHIP and ERα were determined by immunoblotting with anti-CHIP and anti-ERα, respectively. GAPDH was used as an SDS-PAGE loading control. For all experiments, representative results of two independent experiments, each performed in duplicate, are shown.

720 **Fig. 5.** CHIP downregulates ERα-mediated reporter gene expression in HeLa cells.

HeLa cells were plated in 12-well dishes at a density of 1×10^5/well, grown in hormone-free medium for 3 days, and transfected with 10 ng pSG5-ERα, 250 ng ERE-pS2-Luc, 250 ng

various CHIP constructs *(A)* or pBS/U6/CHIPi *(B)*. Twenty four hours after transfection, cells

were treated for 6 hr with DMSO or 10 nM E2 and then assayed for luciferase activity. The

725   ERE-pS2-Luc activity was normalized to SV40-Luc activity, which was determined in a parallel

experiment where ERE-pS2-Luc was replaced with SV40-Luc. The results are expressed as

means ± SE from three independent experiments, with each performed in quadruplicate. P<0.05

(student's t-test, *vs* pcDNA treated with E2) is indicated by an *.

730   **Fig. 6.** CHIP downregulates ERα-mediated gene expression in MCF7 cells.

A. Overexpression of CHIP inhibits ERα—mediated reporter gene expression. MCF7 cells were

plated in 12-well dishes at a density of 1×10^5/well, grown in hormone-free medium for 3 days,

and transfected with 250 ng ERE-pS2-Luc, along with 250 ng various CHIP constructs. Twenty

four hours after transfection, cells were treated with DMSO or 10 nM E2 for 6 hr and then

735   assayed for luciferase. The ERE-pS2-Luc activity was normalized to SV40-Luc activity

(determined in a parallel experiment where ERE-pS2-Luc was replaced with 'SV40-Luc).

Results are expressed as the mean ± SE from three independent experiments, each performed in

quadruplicate. * means P<0.05 (student's t-test, *vs* pcDNA treated with E2). *B. Knockdown of*

CHIP by siRNA increases ERα-mediated reporter gene expression. MCF7 cells were plated as in

740   *(A)* and transfected with 250 ng ERE-pS2-Luc and various amounts (0, 250, and 500 ng) of

pBS/U6/CHIPi. Twenty four hours after transfection, cells were treated and subjected to

luciferase analysis, as in *(A)*. *C. Knockdown of CHIP by siRNA increases expression of pS2*

mRNA. MCF7 cells were plated in 100 mm dishes at a density of 1×10^6/dish, grown in hormone-

free medium for 3 days, and transfected with 5 µg vector or pBS/U6/CHIPi using FuGENE.

745   Forty eight hours after transfection, cells were treated for 6 hr with DMSO or 10 nM E2. The

36

mRNA level of pS2 was determined by real time quantitative PCR. The relative pS2 mRNA levels were normalized with β-actin mRNA and expressed as mean ± SE from three independent experiments, each performed in duplicate. P<0.05 (student's t-test, CHIP-siRNA *vs* pcDNA) is indicated by an *.

750

Fig. 7. Disruption of Hsp90 function induces ERα degradation through a CHIP-dependent mechanism in HeLa cells.

A. CHIP overexpression augments and CHIP depletion by siRNA blocks GA-induced ERα degradation. HeLa cells were plated in 60-mm dishes at a density of $3x10^5$ cells/dish, cultured

755 in hormone-free medium for 3 days, and transfected with 250 ng pSG5-ERα, along with 250 ng pcDNA, pcDNA-His6-CHIP or pBS/U6/CHIPi by using LipofectAMINE Plus Reagent. Twenty four hours after transfection, the cells were treated with 1 μM GA for 0, 0.5, 1 and 3 hr. Cell lysates were immunoblotted with anti-ERα. GAPDH was used as an SDS-PAGE loading control. The band density of exposed films was evaluated with ImageJ software. Relative ERα

760 levels were presented as mean ± SE from three independent experiments. *B. GA enhances CHIP-ERα interaction.* HeLa cells were plated as in *A* and transfected with 250 ng pSG5-ERα and 250 ng pcDNA-His6-CHIP. Twenty four hours after transfection, cells were untreated or treated with 1 μM GA or 10 mM MG132 for 1 hr prior to lysate preparation. ERα protein was precipitated by anti-ERα and the presence of CHIP determined by immunoblotting with anti-

765 His6. The same membrane was then re-probed with anti-ERα to assess the amount of precipitated ERα in the same complex. Representative results of three independent experiments, each performed in duplicate, are shown.

Fig. 8. CHIP is required for geldanamycin-induced ERα degradation in breast cancer MCF7

770   cells.

A. CHIP depletion by CHIP-siRNA eliminates GA-induced ERα degradation. MCF7 cells were

plated in 60-mm dishes at a density of 3×10^5 cells/dish, cultured in hormone-free medium for 3

days, and transfected with 500 ng pcDNA (control) or pBS/U6/CHIPi. Twenty four hours after

transfection, cells were treated with 1 µM GA for 0, 1, 2.5 and 4 hr, and subjected to

775   immunoblotting with anti-ERα. β-tubulin was used as SDS-PAGE loading control. The band

density of exposed films was evaluated with ImageJ software. Relative ERα levels are presented

as mean ± SE from three independent experiments (lower panel). *B. GA stimulates CHIP-ERα*

interaction. MCF7 cells were plated at 1×10^6 cells in 100-mm dishes, cultured in hormone-free

medium for 3 days, and treated with 1 µM GA for 0, 1 and 3 hr prior to lysate preparation. ERα

780   protein was precipitated by anti-ERα and the presence of CHIP examined by immunoblotting

with anti-CHIP. The same membrane was then reprobed with ERα antibody to assess the

amount of precipitated ERα in the same complex. Representative results of two independent

experiments, each performed in duplicate, are shown.

785   **Fig. 9.** Effect of ligand binding on geldenamycin-induced ERα degradation

A. ERα protein levels in MCF7 cells treated with GA before or after ligand exposure. MCF7

cells were plated in 60-mm dishes at a density of 3×10^5 cells/dish and cultured in hormone-free

medium for 3 days. *Upper panel,* cells were treated with vehicle, 10 nM E2, 1 µM OHT, 100

nM ICI or 1 µM GA for 6 hr; *Middle panel,* cells were exposed to indicated ligand for 30 min

790   prior to a 6-hr GA treatment; *Lower panel*, 30 min after GA treatment, cells were exposed to

indicated ligand for 5.5 hr. For all experiments, ERα levels were determined by immunoblotting

with anti-ERα. β-tubulin was used as SDS-PAGE loading control. B. *Effect of ligands on GA-*

induced CHIP-ERα interaction. MCF7 cells were plated in 100-mm dishes at a density of 1×10^6

cells/dish, cultured in hormone-free medium for 3 days, and then transfected with 5 µg pcDNA-

795   His6-CHIP by using FuGENE. Twenty four hours after transfection, the cells were treated with

1 µM GA for 30 min, followed by a 30-min treatment with indicated ligands (100 nM E2, 1 µM

OHT and 100 nM ICI). ERα protein from the cell lysates was precipitated using anti-ERα.

CHIP presence in the precipitated ERα complex was determined by immunoblotting with anti-

His6. The same membrane was re-probed with ERα antibody to assess the amount of

800   precipitated ERα. Representative results of two independent experiments, each performed in

duplicate, are shown.

Fig. 10. Effect of CHIP and geldanamycin on ERα cellular localization.

HeLa cells were plated in 6-well dishes at a density of 1×10^5 cells/dish, cultured in hormone-free

805   medium for 3 days, and transfected with 250 ng GFP-ERα and 250 ng pcDNA or pcDNA-His6-

CHIP by using LipofectAMINE Plus Reagent. Twenty four hours after transfection, the

transfected cells were treated with 1 µM GA or 100 nM ICI for 6 hr. The fluorescence of GFP-

ERα was then examined using an inverted microscope (Axiovert 40 CFL) *(A)*. The number of

cells expressing GFP-ERα from 10 microscope fields was present in the histogram *(B)*.

810   Representative results of two independent experiments, each performed in triplicate, are shown.

Open bar, vehicle-treated controls; Gray bar, GA treatment (1 µM, 6 h).

Fig. 11. Schematic summary of distinct ERα degradation pathways.

Nascent ERα is translocated into nucleus. There, by associating with Hsp90, the receptor is
maintained in a ligand-binding competent conformation, ready for subsequent activation. In the
absence of ligand or other activation signals, CHIP constantly targets Hsp90-associated ERα for
degradation. Ligand binding disassembles the ERα-Hsp90 complex and thus protects ERα from
CHIP-mediated degradation. However, depending upon the ligand, distinct downstream
destructive pathways are engaged in the degradation of liganded ERα. When activated by E2,
ERα is degraded through a transcription-coupled mechanism. In response to ICI, nuclear ERα-
ICI complex is immobilized to the nuclear matrix and undergoes rapid proteasomal degradation.
In addition, ICI induces cytoplasmic retention and aggregation of nascent ERα OHT-ERα
complexes are stable, likely due to the lack of transcriptional activity.

815

820

40
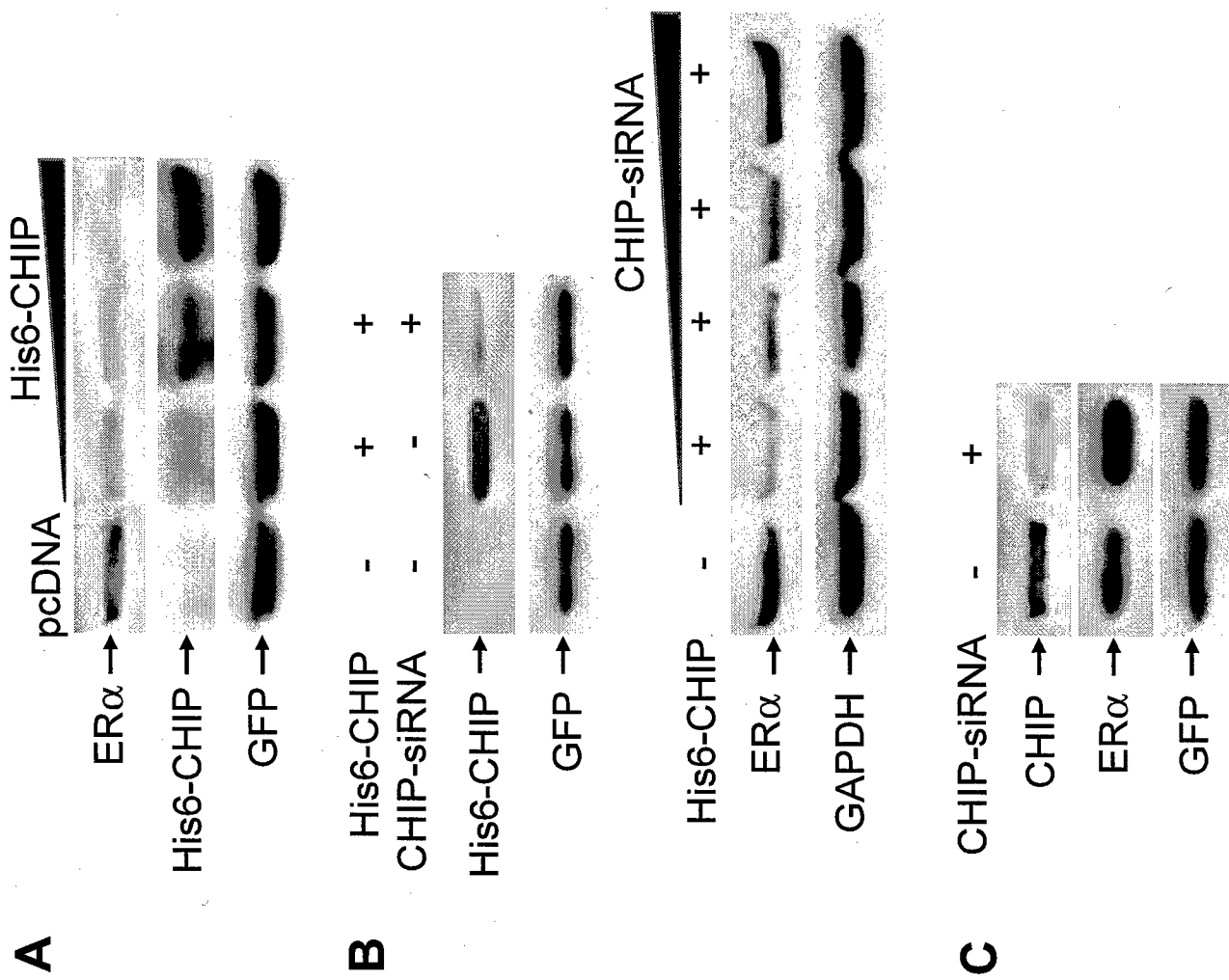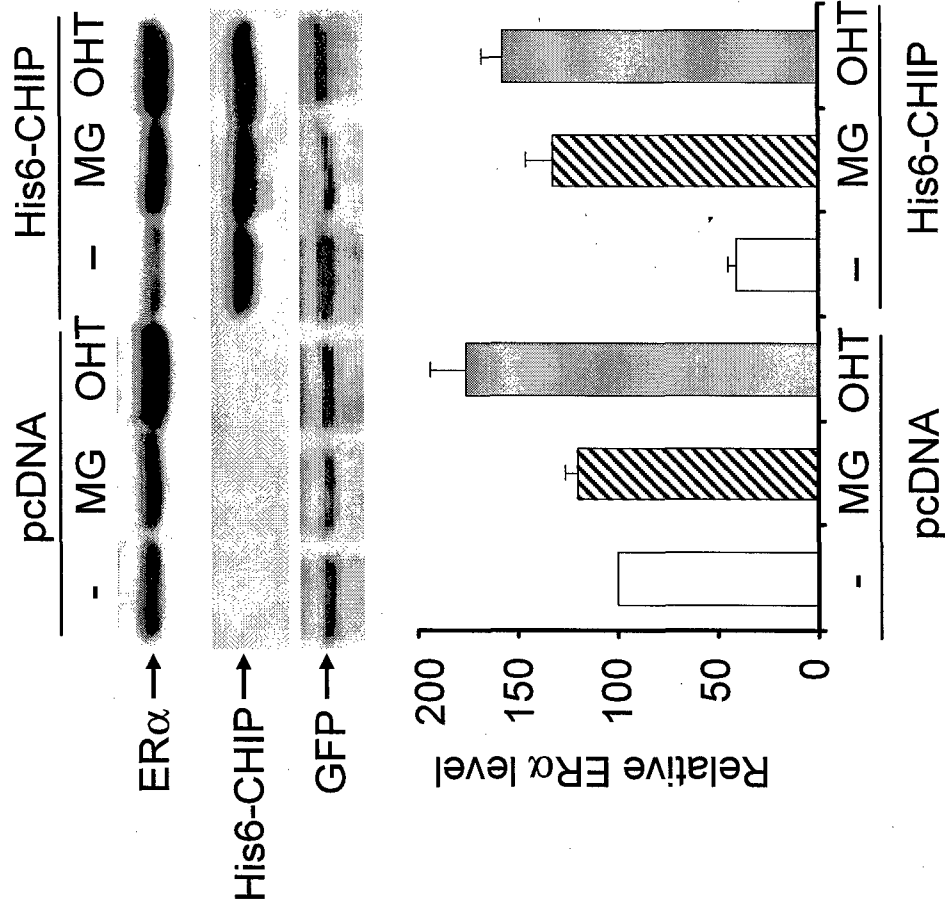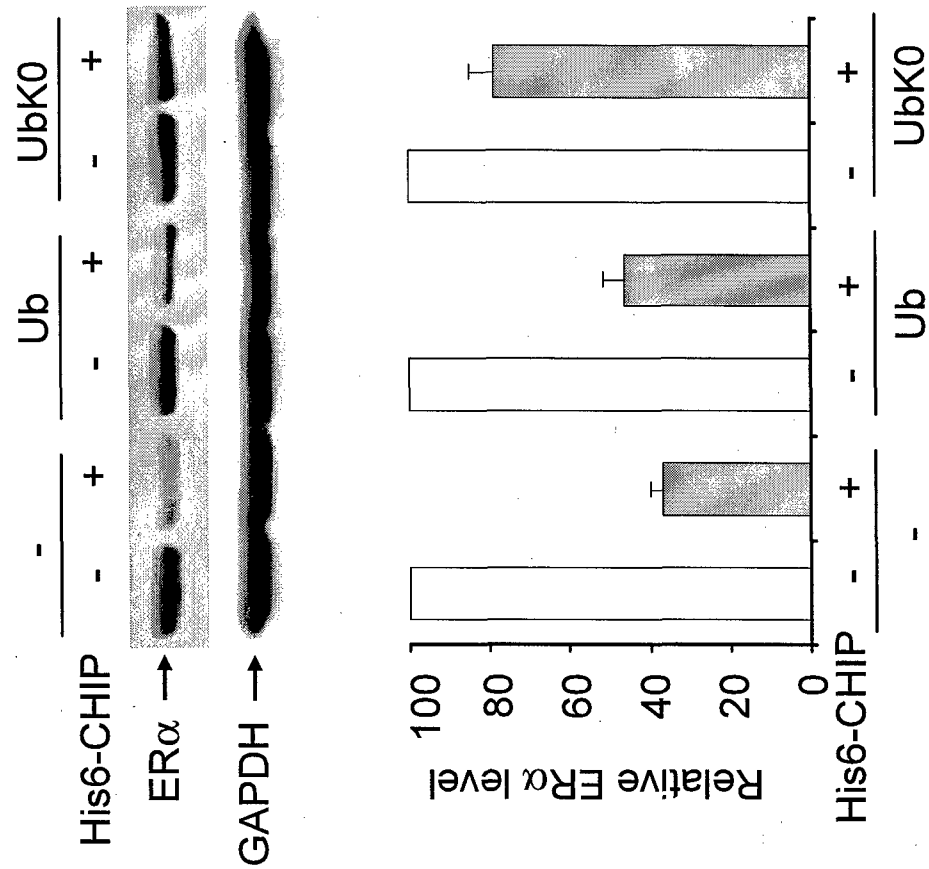
Fig. 1

Fig. 2
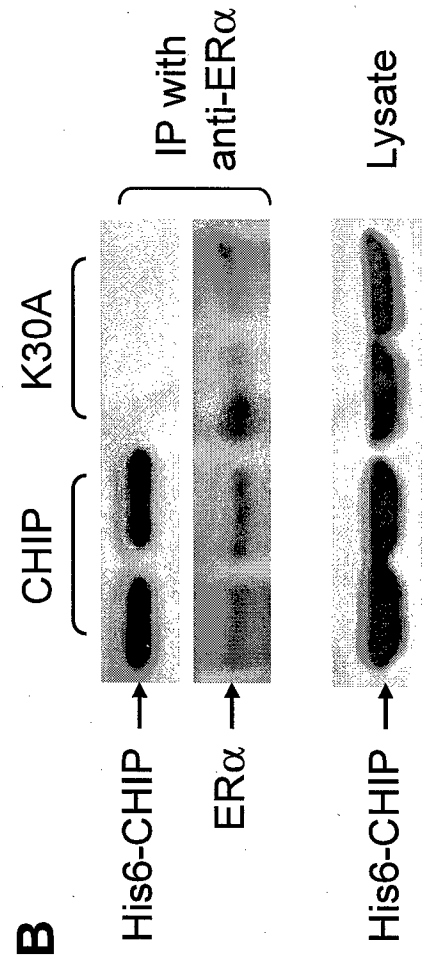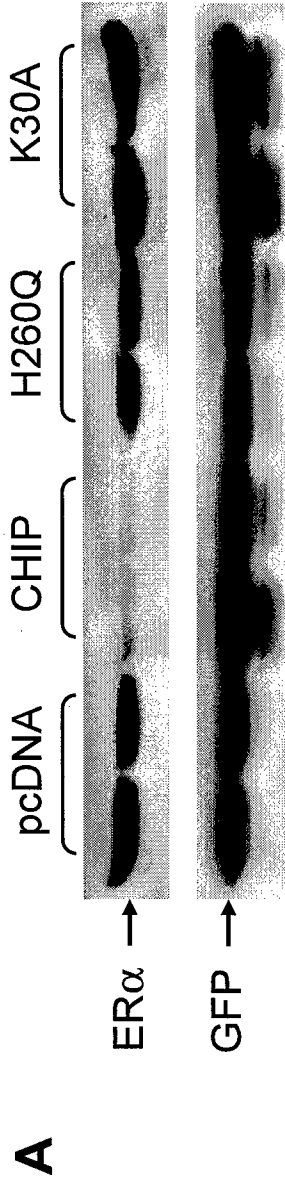
Fig. 3
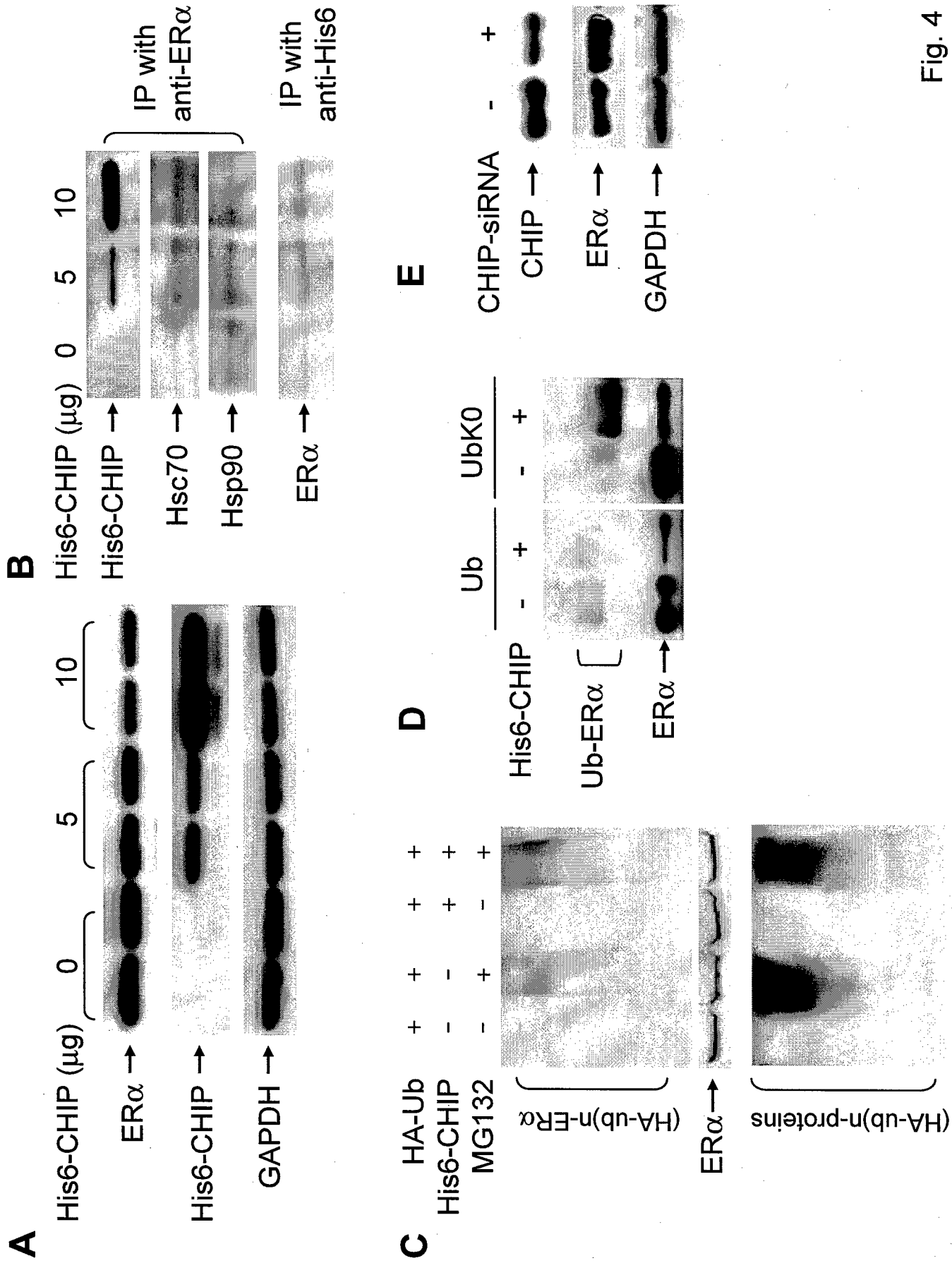
Fig. 4
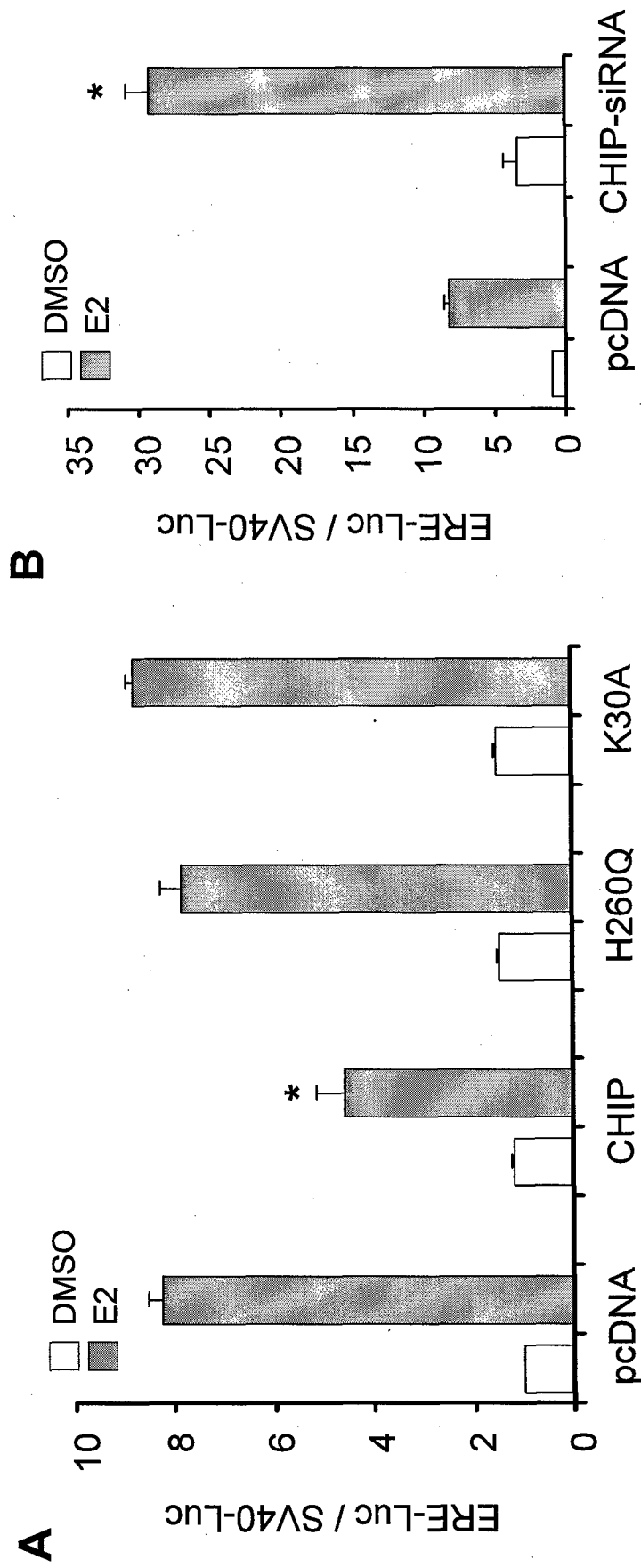
Fig. 5
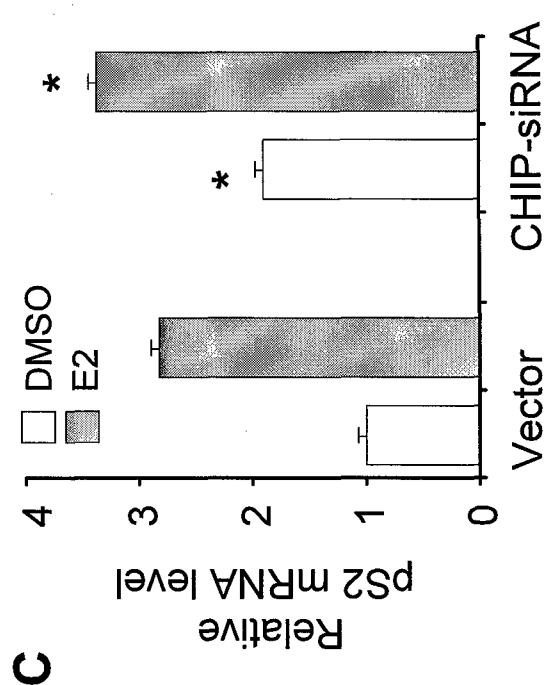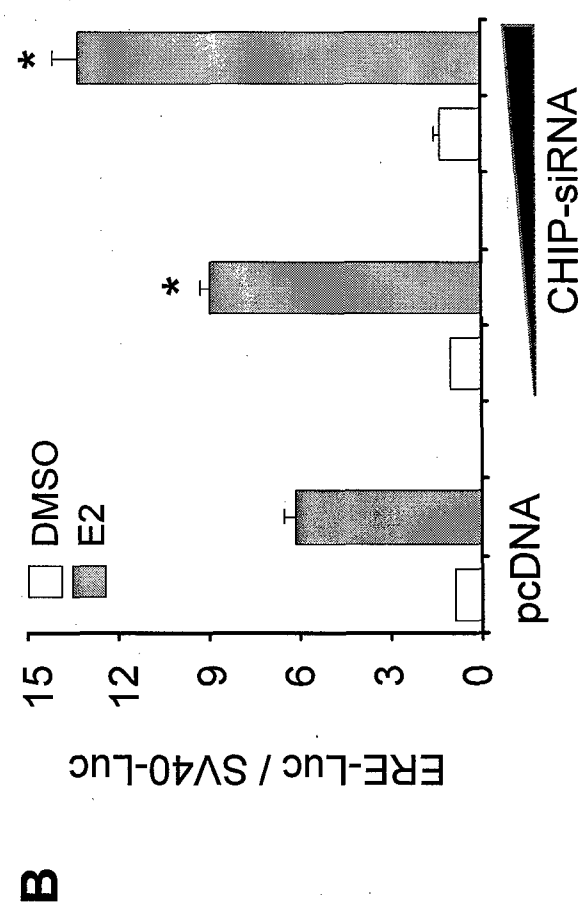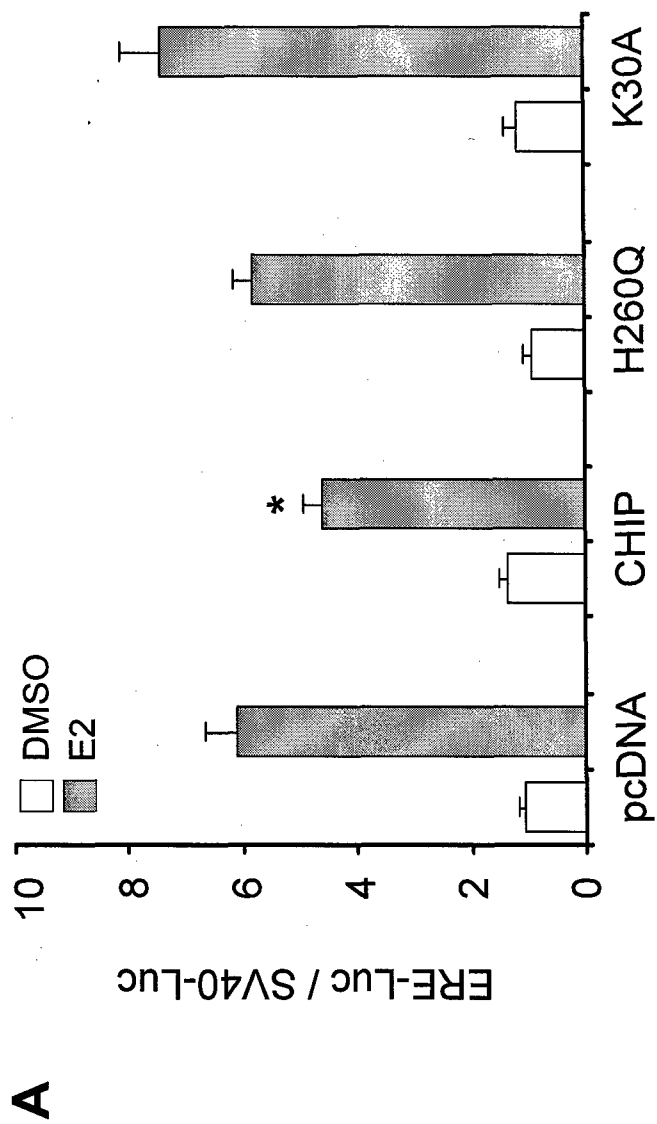
Fig. 6
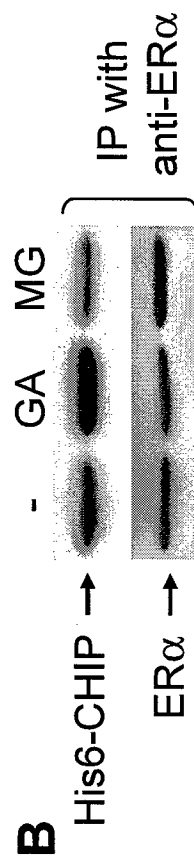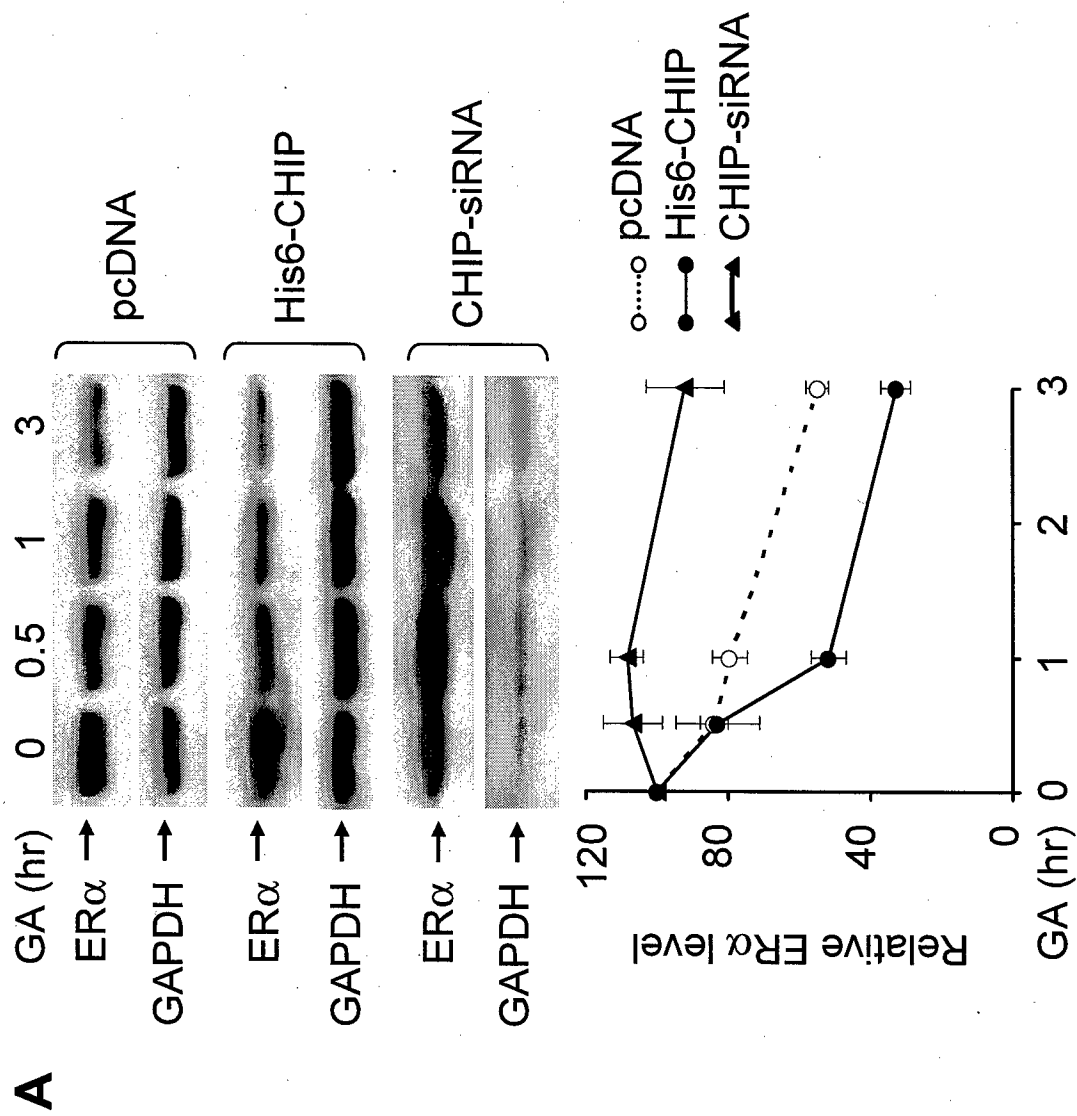
Fig. 7
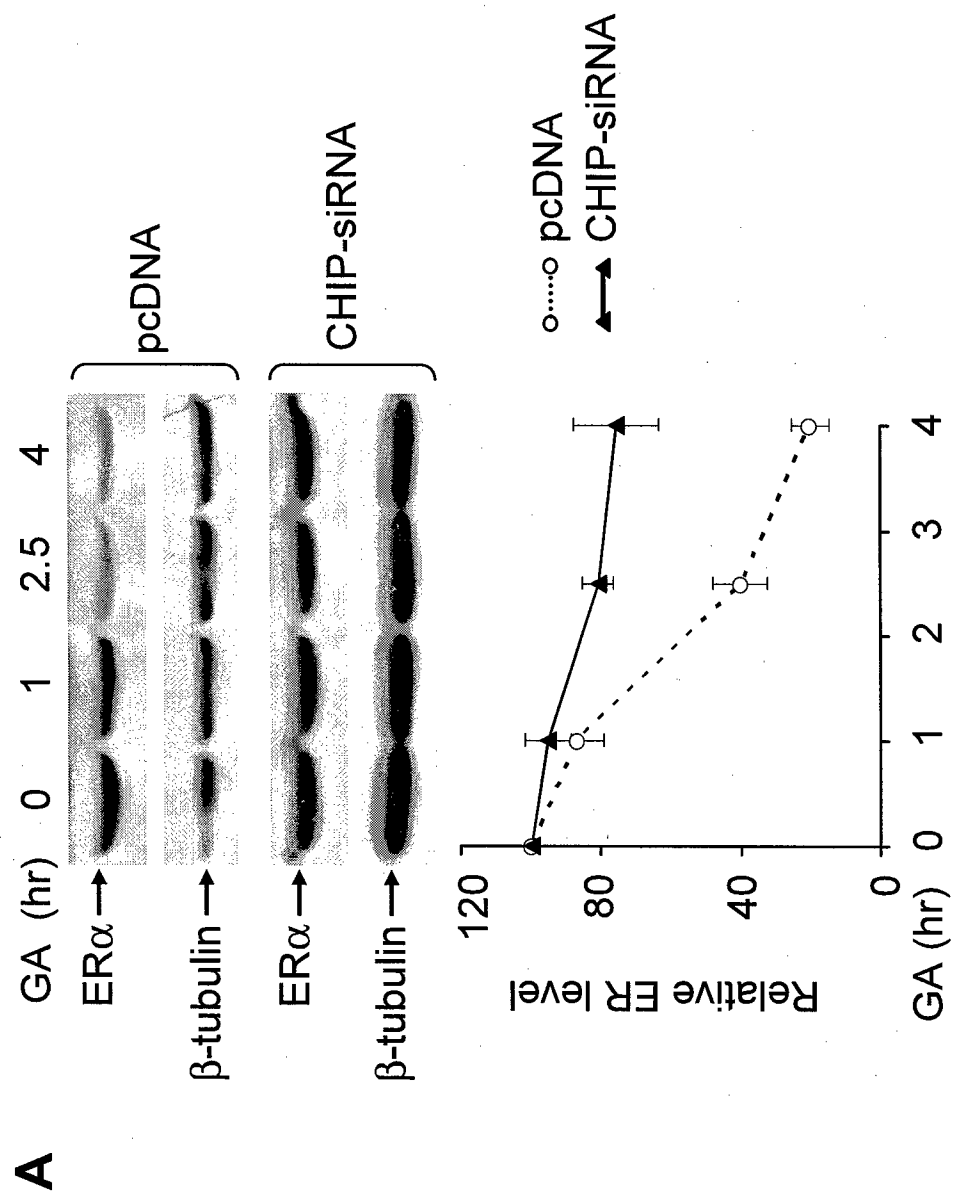
Fig. 8

Fig. 9

Fig. 10

Fig. 11

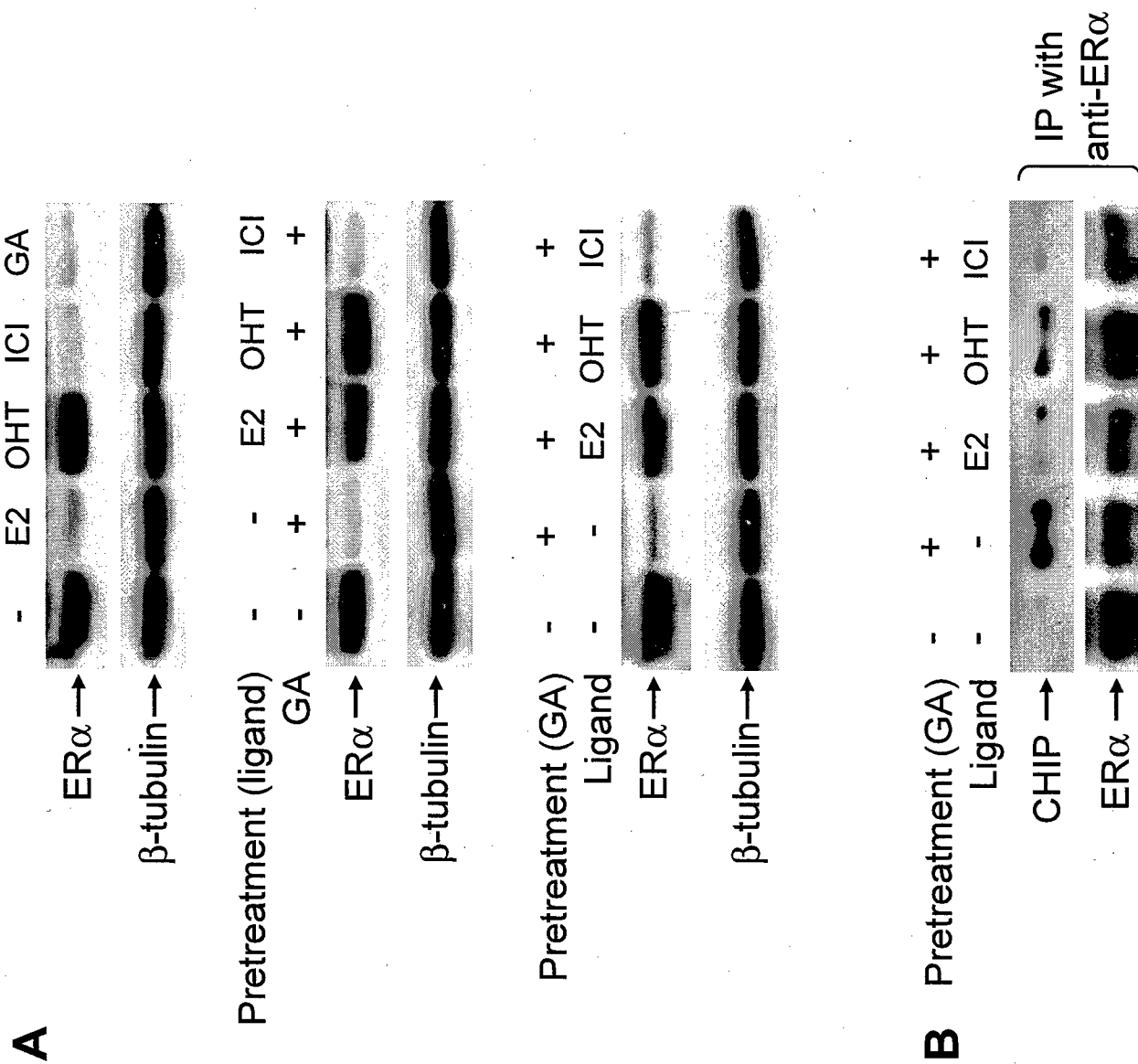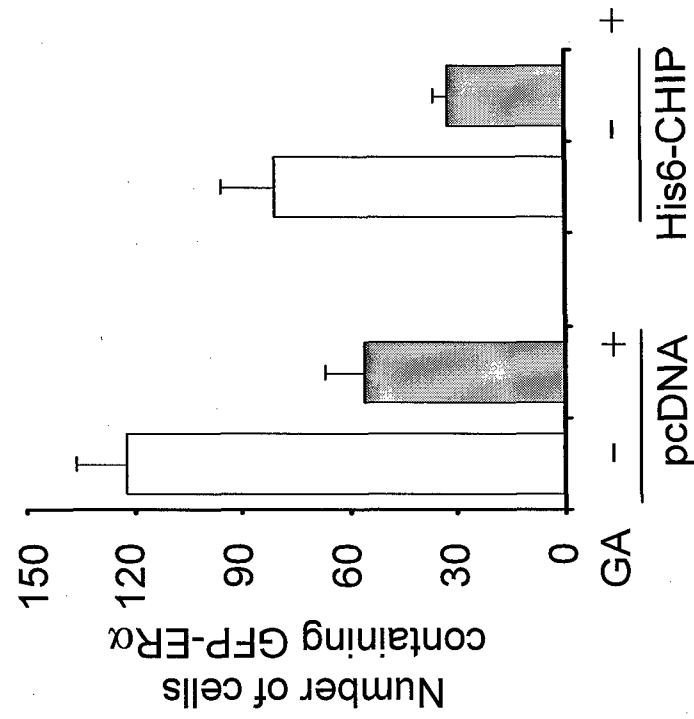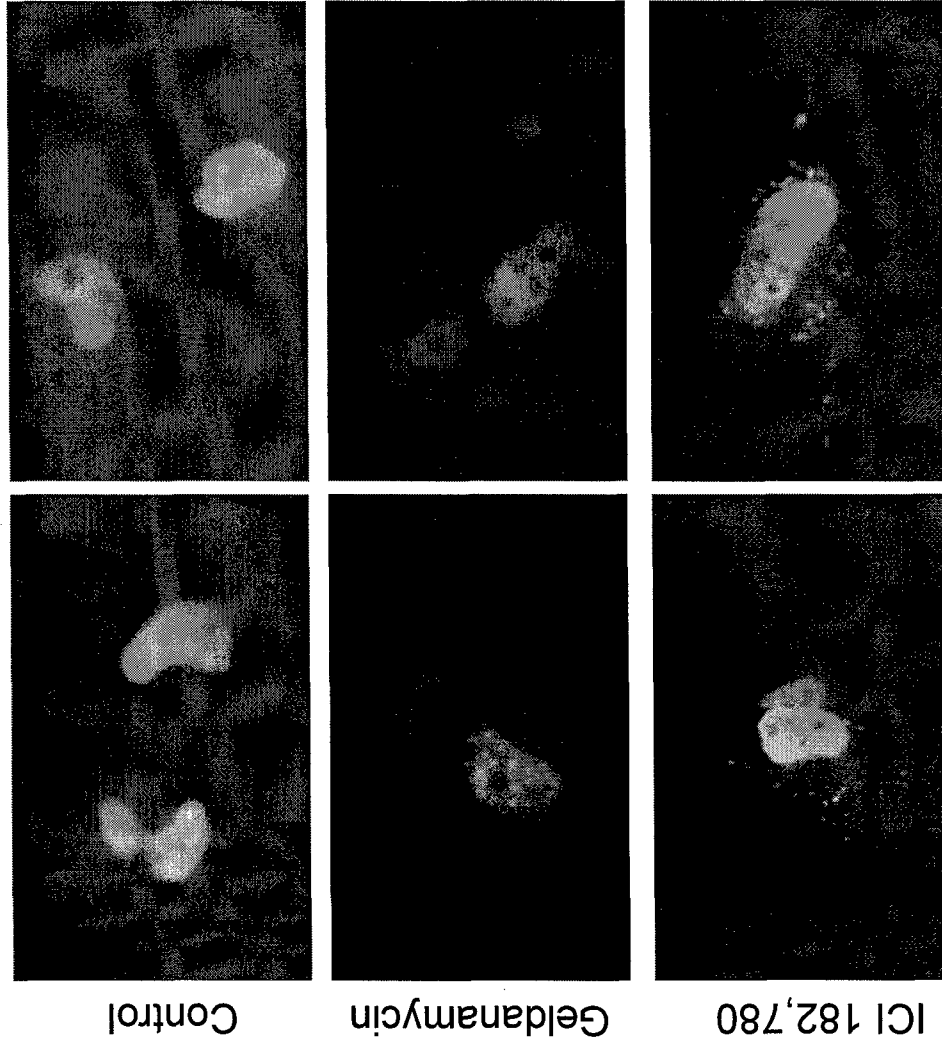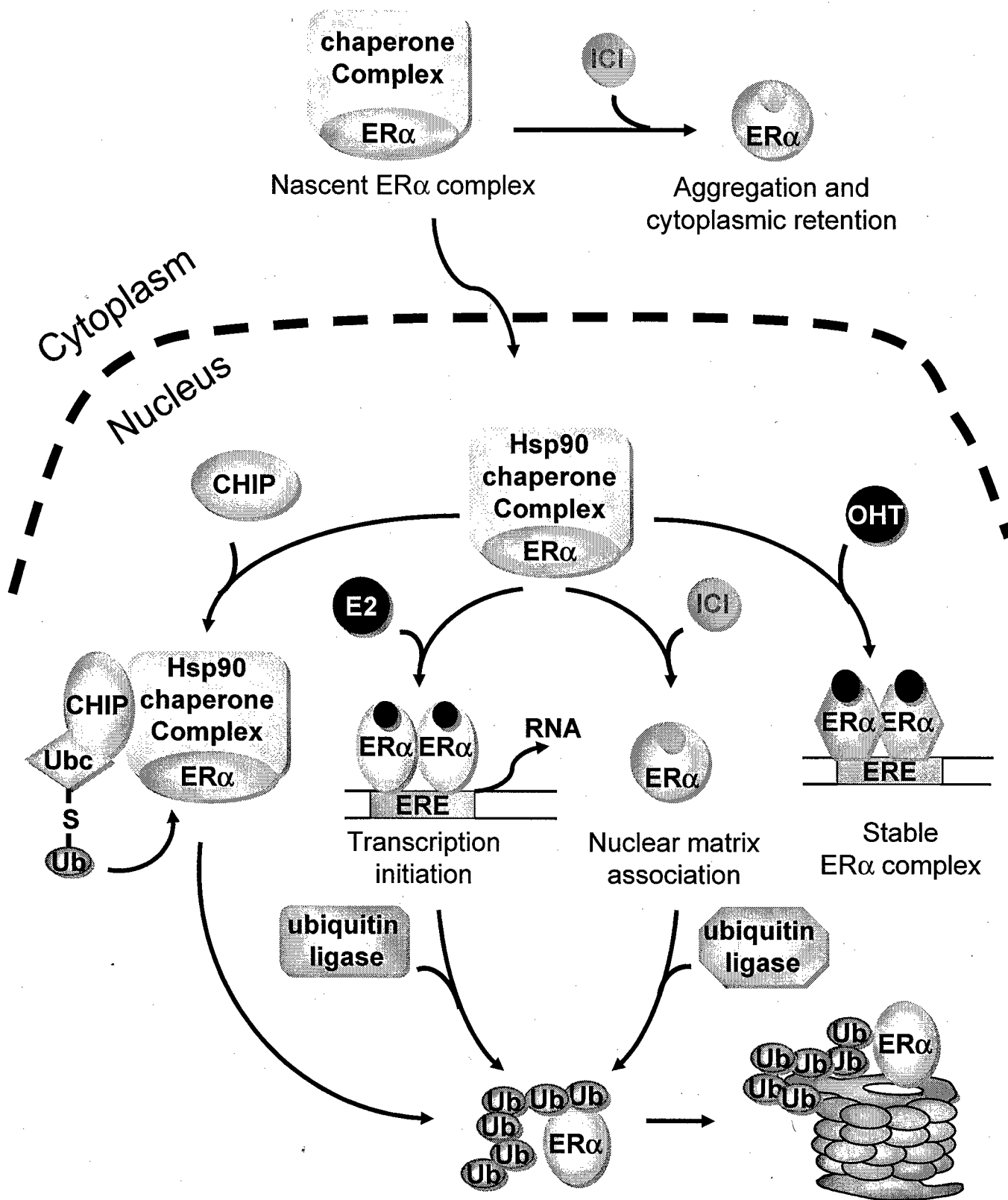# Loss of Estrogen Receptor Signaling Triggers Epigenetic Silencing of Downstream Targets in Breast Cancer

Yu-Wei Leu,[1] Pearlly S. Yan,[1] Meiyun Fan,[2,3] Victor X. Jin,[1] Joseph C. Liu,[1] Edward M. Curran,[4] Wade V. Welshons,[4] Susan H. Wei,[1] Ramana V. Davuluri,[1] Christoph Plass,[1] Kenneth P. Nephew,[2,3] and Tim H-M. Huang[1]

[1]Human Cancer Genetics Program, Department of Molecular Virology, Immunology, and Medical Genetics, Comprehensive Cancer Center, The Ohio State University, Columbus, Ohio; [2]Medical Sciences, Indiana University School of Medicine, Bloomington, Indiana; [3]Department of Cellular and Integrative Physiology and Obstetrics and Genecology, Indiana University Cancer Center, Indianapolis, Indiana; and [4]Department of Veterinary Biomedical Sciences, University of Missouri, Columbia, Missouri

ABSTRACT

Alterations in histones, chromatin-related proteins, and DNA methylation contribute to transcriptional silencing in cancer, but the sequence of these molecular events is not well understood. Here we demonstrate that on disruption of estrogen receptor (ER) α signaling by small interfering RNA, polycomb repressors and histone deacetylases are recruited to initiate stable repression of the *progesterone receptor (PR)* gene, a known ERα target, in breast cancer cells. The event is accompanied by acquired DNA methylation of the *PR* promoter, leaving a stable mark that can be inherited by cancer cell progeny. Reestablishing ERα signaling alone was not sufficient to reactivate the *PR* gene; reactivation of the *PR* gene also requires DNA demethylation. Methylation microarray analysis further showed that progressive DNA methylation occurs in multiple ERα targets in breast cancer genomes. The results imply, for the first time, the significance of epigenetic regulation on ERα target genes, providing new direction for research in this classical signaling pathway.

INTRODUCTION

The steroid hormone estrogen is important for normal breast development, but it is also important for growth and progression of breast cancer. The molecular actions of estrogen are mediated by estrogen receptors (ERs), ERα and ERβ. On ligand binding, ERα functions as a transcription factor by either binding to DNA targets or tethering to other transcription factors, such as AP-1 and SP-1 (1). These molecular interactions have been shown to positively or negatively modulate the activity of ERα downstream genes important to breast epithelial development.

It is known that estrogen signaling regulates the growth of some breast tumors, and antiestrogen therapies can effectively block this growth signaling, resulting in tumor suppression (2). However, most tumors eventually develop resistance to this endocrine therapy, and antiestrogens are mostly ineffective in patients with advanced disease (2). Mechanisms underlying this hormonal resistance are complex, involving intricate interactions between ERα and kinase networks (1, 2). In addition, epigenetic silencing of *ERα* is known to contribute to the antiestrogen resistance (1, 2). An emerging theme not yet investigated in this field is the subsequent influence on the expression of ERα downstream target genes.

Epigenetics can be defined as the study of heritable changes that modulate chromatin organization without altering the corresponding DNA sequence. DNA methylation, the addition of a methyl group to the fifth carbon position of a cytosine residue, occurs in CpG dinucleotides (3) and is a key epigenetic feature of the human genome. These dinucleotides are usually aggregated in stretches of 1- to 2-kb GC-rich DNA, called CpG islands, located in the promoter and first exon of ~60% of human genes (3, 4). Promoter methylation is known to participate in reorganizing chromatin structure and also plays a role in transcriptional inactivation (3, 5). Studies have suggested that the CpG island in an active promoter is usually unmethylated, with the surrounding chromatin displaying an "open" configuration, allowing for the access of transcription factors and other coactivators to initiate gene expression (6–8). Furthermore, transcription factor occupancy may make the promoter inaccessible to repressors or other chromatin-remodeling proteins. In contrast, the CpG island in an inactive promoter may become methylated, with the associated chromatin exhibiting a "closed" configuration. As a result, the methylated area is no longer accessible to transcription factors, disabling the functional activity of the promoter (7, 9, 10).

Recent studies have shown that establishing transcriptional silencing of a gene involves a close interplay between DNA methylation and histone modifications (7, 11). This process may be achieved by recruiting histone-modifying enzymes, such as histone deacetylases, which mediate posttranslational modification at the NH_2 terminus ends of histones (7, 11). As a result, chromatin modifications form distinct patterns, known as the "histone code," that may dictate gene expression (12–14).

Two models have been offered to describe the molecular sequence leading to the establishment of epigenetic gene silencing. One model suggests that histone modifications are the primary initiating event in transient repression (15, 16). DNA methylation subsequently accumulates in the targeted CpG island, creating a heterochromatin environment to establish a heritable, long-term state of transcriptional silencing. However, a second model is that DNA methylation can actually specify unique histone codes for maintaining the silenced state of a gene (17–20). In this case, DNA methylation may precede histone modifications. Clearly, this epigenetic process is complex, and multiple systems may be implemented for genes participating in different signaling pathways.

In this study, we investigated whether the removal of ERα signaling triggers changes in DNA methylation and chromatin structure of ERα target promoters. By using RNA interference (RNAi) to transiently disable ERα in breast cancer cells, we show, for the first time, that polycomb repressors and histone deacetylases assemble on the promoters of interrogated ERα target genes to participate in long-term transcriptional silencing. These events are later accompanied by a progressive accumulation of DNA methylation in the promoter re-

Note: Supplementary data for this article can be found at Cancer Research Online (http://cancerres.aacrjournals.org). T. Huang is a consultant to Epigenomics, Inc., Berlin, Germany.

Requests for reprints: Tim H-M. Huang, Human Cancer Genetics Program, Department of Molecular Virology, Immunology, and Medical Genetics, Comprehensive Cancer Center, The Ohio State University, 420 West 12th Avenue, Columbus, OH 43210. Phone: 614-688-8277; Fax: 614-292-5995; E-mail: huang-10@medctr.osu.edu.

gions of the now silent targets, leaving a heritable "mark" that may be stably transmitted to cell progeny.

MATERIALS AND METHODS

Cell Lines and Clinical Samples. The breast cancer cell line MCF-7 and its derived subline, C4-12, were routinely maintained in our laboratories. For the demethylating treatment, cells were plated at a density of 2×10^6 cells per 10-cm dish and pretreated with 2 or 5 μmol/L 5-aza-2'-deoxycytidine (5-AzadC; Sigma, St. Louis, MO) for 5 days before treatment with 17β-estradiol (E$_2$; 10 nmol/L, 24 hours). Thirty-two invasive ductal carcinomas were obtained from patients undergoing breast surgery at the Ellis Fischel Cancer Center (Columbia, MO), in compliance with the institutional review board. Seven tumor-free breast parenchymas were used as controls. The ER status of tumor tissue was determined by immunohistochemical staining (21).

Transfection of Estrogen Receptor α Small Interfering RNAs. MCF-7 cells (60% confluent in a 3.5-cm–diameter culture dish) were starved in serum-free medium (minimal essential medium only) for 72 hours, followed by the addition of 10 nmol/L E$_2$ (E2758; Sigma) for 24 hours. The cells were then transfected with small interfering RNAs (siRNAs) for 4 to 5 hours with DMRIE-C reagent (Invitrogen, Carlsbad, CA). Double-stranded siRNA was generated using the *Silencer* siRNA Construction Kit (Ambion, Austin, TX). The siRNA oligonucleotides designed according to the ERα mRNA sequence (GenBank accession numbers AF_258449, 258450, and 258451) are as follows: (*a*) target sequence 1 (5'-AACCTCGGGCTGTGCTCTTTT), sense strand siRNA primer 5'-CCTCGGGCTGTGCTCTTTTTTCCTGTCTC and antisense strand siRNA primer AAAAGAGCACAGCCCGAGGTTCCTG-TCTC; and (*b*) target sequence 17 (5'-AAACAGGAGGAAGAGCTGCCA), sense strand siRNA primer 5'-ACAGGAGGAAGAGCTGCCATTCCT-GTCTC and antisense strand siRNA primer 5'-TGGCAGCTCTTCCTCCT-GTTTCCTGTCTC.

Media were changed after transfection. The cells were then harvested for total RNA (RNeasy Kit; Qiagen, Valencia, CA) and genomic DNA (QIAamp; Qiagen) isolation at various time periods after siRNA treatment.

Transfection of Estrogen Receptor α Expression Vector. C4-12 cells were transfected with pcDNA-ERα (C4-12/ER) or empty vector (C4-12/vec) using LipofectAMINE Plus Reagent (Life Technologies, Inc., Carlsbad, CA) and then exposed to an antibiotic (G418; 0.5 mg/mL) for 3 weeks. Expression of ERα in G418-resistant colonies was detected by immunoblotting with an anti-ER antibody (Chemicon, Temecula, CA).

Real-Time Reverse Transcription-Polymerase Chain Reaction. Total RNA (2 μg) was treated with DNase I to remove potential DNA contamination and then reverse transcribed using the SuperScript II reverse transcriptase (Invitrogen). Real-time polymerase chain reactions (PCRs) were then performed using puReTaq Ready-To-Go PCR beads (Amersham Biosciences, Piscataway, NJ) and monitored by SYBR Green I (BioWhittaker, Walkersville, MD) using a Smart Cycler Real-Time PCR instrument (Cepheid, Sunnyvale, CA) for 42 cycles. PCR products of the expected size were also visualized on agarose gels stained with ethidium bromide. Alternatively, the reverse transcription-PCR (RT-PCR) reaction was conducted using iQ SYBR Green Supermix (Bio-Rad, Hercules, CA) in an iCycler system (Bio-Rad) for *PR* transcripts (22). The relative mRNA level of a given locus was calculated by Relative Quantitation of Gene Expression (Applied Biosystems, Foster City, CA) with *glyceraldehyde-3-phosphate dehydrogenase* (*GAPDH*) or β-actin mRNA as an internal control. The primers used for RT-PCR reactions are listed in Supplementary Table S1.

Immunofluorescence and Western Blot Analysis. MCF-7 cells (2×10^5) treated with or without ERα siRNAs were permeablized with 0.5% Nonidet P-40/PBS and blocked with a 1:100 dilution of horse serum before incubation with primary anti-ERα antibody (1:1,000; mouse monoclonal antibody D-12; Santa Cruz Biotechnology, Santa Cruz, CA). Sample slides were washed with PBS and incubated in the dark with secondary antibody (1:500) conjugated with Texas Red (fluorescent antimouse IgG kit; Vector Laboratories, Burlingame, CA) for 1 hour. The slides were then mounted with Vectashield mounting medium with 4',6-diamidino-2-phenylindole (Vector Laboratories) and observed under a fluorescence microscope (Zeiss Axioskop 40; Zeiss, Thornwood, NY). Images were captured by the AxioCam HRC camera and analyzed by AxioVision 5.05 software.

Small interfering RNA-treated cells and control cells were lysed in the presence of proteinase inhibitors. One hundred micrograms of protein were subjected to 7% SDS-PAGE and transferred to immunoblot membranes. The membranes were then incubated with mouse anti-ERα (MAB463; Chemicon) and labeled secondary antibody. GAPDH was used a loading control.

Chromatin Immunoprecipitation-Polymerase Chain Reaction. Cultured cells (2×10^6) were cross-linked with 1% formaldehyde and then washed with PBS in the presence of protease inhibitors. The cells were resuspended in lysis buffer, homogenized using a tissue grind pestle to release nuclei, and then pelleted by centrifugation. SDS-lysis buffer from a chromatin immunoprecipitation (ChIP) assay kit (Upstate Biotechnology, Lake Placid, NY) was used to resuspend the nuclei. The lysate was sonicated to shear chromatin DNAs and then centrifuged to remove cell debris. The supernatants were transferred to new tubes and incubated overnight with an antibody against ERα, YY-1, or EZH2 (Santa Cruz Biotechnology); HDAC1, MBD2, or MeCP2 (Upstate Biotechnology); and DMNT1, DNMT3a, or DNMT3b (Imgenex, San Diego, CA). Agarose slurry was then added to the mixture, and the chromatin-bound agarose was centrifuged. The supernatant was collected and used for total input (it serves as a positive control) in the ChIP-PCR assay. After elution, proteins were digested from the bound DNA with proteinase K. Phenol/chloroform-purified DNA was then precipitated and used in ChIP-PCR assays for a *progesterone receptor* (*PR*) promoter region. The primer sequences were 5'-GGCTTTGGGCGGGGCCTCCCTA (sense strand) and 5'-TCTGCTGGCTCCGTACTGCGG (antisense strand). After amplification, ^{32}P-incorporated PCR products were separated on 8% polyacrylamide gels and subjected to autoradiography using a Storm PhosphorImager (Amersham Biosciences).

Methylation-Specific Polymerase Chain Reaction. Genomic DNA (1 μg) from each sample was bisulfite-converted using the EZ DNA Methylation Kit (Zymo Research Corp., Orange, CA), according to the manufacturer's protocol. The converted DNA was eluted with 40 μL of elution buffer and then diluted 50 times for methylation-specific PCR (MSP). The primer sets designed for amplifying the methylated or unmethylated allele of the PR locus are listed in Supplementary Table S2. All PCR reactions were performed in PTC-100 thermocyclers (MJ Research, Watertown, MA) using AmpliTaq Gold DNA polymerase (Applied Biosystems). ^{32}P-incorporated amplified products were separated on 8% polyacrylamide gels and subjected to autoradiography using a Storm PhosphorImager (Amersham Biosciences).

Combined Bisulfite Restriction Analysis. Combined bisulfite restriction analysis (COBRA) was carried out essentially as described previously (23). Bisulfite-modified DNA ($\sim$10 ng) was used as a template for PCR with specific primers flanking the interrogated sites (*Taq*I or *Bst*UI) of an ERα downstream target. Primer sequences used for amplification are listed in Supplementary Table S3. After amplification, radiolabeled PCR products were digested with *Taq*I or *Bst*UI, which restrict unconverted DNA containing methylated sites. The undigested control and digested DNA samples were run in parallel on polyacrylamide gels and subjected to autoradiography. The percentage of methylation was determined as the intensity of methylated fragments relative to the combined intensity of unmethylated and methylated fragments.

Chromatin Immunoprecipitation on Chip. MCF-7 cells (2×10^7) were used to conduct ChIP with an antibody specific for ERα following the protocol described (see Chromatin Immunoprecipitation-Polymerase Chain Reaction). After chromatin coimmunoprecipitation, DNA was labeled with Cy5 fluorescence dye and hybridized to a genomic microarray panel containing $\sim$9,000 CpG islands (24). Microarray hybridization and posthybridization washes have been described previously (25). The washed slides were scanned by a Gene Pix 4000A scanner (Axon, Union City, CA), and the acquired microarray images were analyzed with GenePix Pro 4.0 software. This ChIP-on-chip experiment was conducted twice.

Positive CpG island clones were sequenced, and the derived sequences were used to identify putative transcription start sites by Blastn[5] or Blat.[6] Both Genomatrix[7] and TFSEARCH[8] programs were then used to localize the consensus sequences of the estrogen response elements (EREs) and other

---

[5] http://www.ncbi.nlm.nih.gov/BLAST/.
[6] http://genome.cse.ucsc.edu/cgi-bin/hgBlat.
[7] http://www.genomatix.de/site_map/index.html.
[8] http://www.cbrc.jp/research/db/TFSEARCH.html.

related transcription factor binding sites (AP-1, SP-1, cAMP-responsive element binding protein, and CEBP).

Differential Methylation Hybridization. Differential methylation hybridization (DMH) was performed essentially as described previously (25, 26). Briefly, 2 μg of genomic DNA were digested by the 4-base frequent cutter *Mse*I, which restricts bulk DNA into small fragments but retains GC-rich CpG island fragments (24). H-24/H-12 PCR linkers (5'-AGGCAACTGTGCTATC-CGAGGGAT-3' and 5'-TAATCCCTCGGA-3') were then ligated to the digested DNA fragments. The DNA samples were further digested with two methylation-sensitive endonucleases, *Hpa*II and *Bst*UI, and amplified by PCR reaction using H-24 as a primer. After amplification, test DNA from siRNA-treated cell lines or clinical samples was labeled with Cy5 (red) dye, whereas control DNA from the mock-transfected cell lines or normal female blood samples was coupled with Cy3 (green) dye. Equal amounts of test and control DNAs were cohybridized to a microarray slide containing 70 ERα promoter targets (average, 500 bp) identified from the ChIP-on-chip results. Posthybridization washing and slide scanning are described above. Normalized Cy5/Cy3 ratios of these loci were calculated by GenePix Pro 4.0.

Shrunken Centroids Analysis. DMH microarray data were analyzed by the procedure described online.[9] This program incorporates graphic methods for automatic threshold choice and centroid classification.

Statistical Analyses. Differences of methylation or mRNA levels in experimental studies were analyzed by a paired t test. Methylation differences between two tumor groups were determined with a Pearson's χ^2 test. $P < 0.05$ was considered statistically significant.

RESULTS

RNA Interference Transiently Knocks Down Estrogen Receptor α Expression in Breast Cancer Cells. Although several *in vitro* systems and mouse models are available for analysis of estrogen signaling, to our knowledge, the recently described RNAi (27) has not been actively used in this area of research. We therefore used this technology to specifically repress *ER*α gene expression via targeted RNA degradation (28, 29). Six different *ER*α siRNAs, two of which have sequences homologous to a splice variant, were synthesized (Fig. 1*A*). These siRNAs (40 nmol/L) were individually transfected into MCF-7, an ERα-positive human breast cancer cell line. MCF-7 cells were cultured in the presence of E$_2$. Quantitative RT-PCR analysis showed that, 24 hours after transfection, two siRNAs, siRNAs 1 and 17, were capable of repressing ERα transcripts (Fig. 1*B*). Specifically for siRNA 1, we observed a >93% decrease of *ER*α mRNA. Immunofluorescence (Fig. 1*C*) and Western blot (Fig. 1*D*) analyses confirmed that this RNAi also dramatically reduced ERα protein synthesis. This inhibitory effect appeared to be transient, and the expression of ERα protein reappeared in cultured cells 4 weeks after RNAi withdrawal (Fig. 1*D*).

Epigenetic Silencing of the *PR* Gene Is Triggered by Estrogen Signal Disruption. We hypothesized that disruption of ERα signaling by siRNA may lead to the silencing of some positively regulated ERα targets governed by epigenetic mechanisms. To this end, a known ERα downstream target, the *PR* gene, was investigated in detail. In Fig. 2*A* and *B*, quantitative RT-PCR analysis showed that by 36 hours after treatment of MCF-7 cells with siRNA 1, the level of *PR* transcripts (PR-A and PR-B) was reduced by >95% (paired t test, $P < 0.0001$). Next, ChIP-PCR was performed to determine the status of chromatin remodeling at the 5'-end of the *PR* gene. The protein-DNA complexes were immunoprecipitated with antibodies to ERα or to specific modified histones (acetyl-H3, acetyl-H3-K9, and methyl-H3-K4) known to specify active transcription (7, 30). As shown in Fig. 2*C*, the presence of these active chromatin components was diminished over a period of 36 hours, coinciding with decreased ERα binding to the *PR* promoter region.
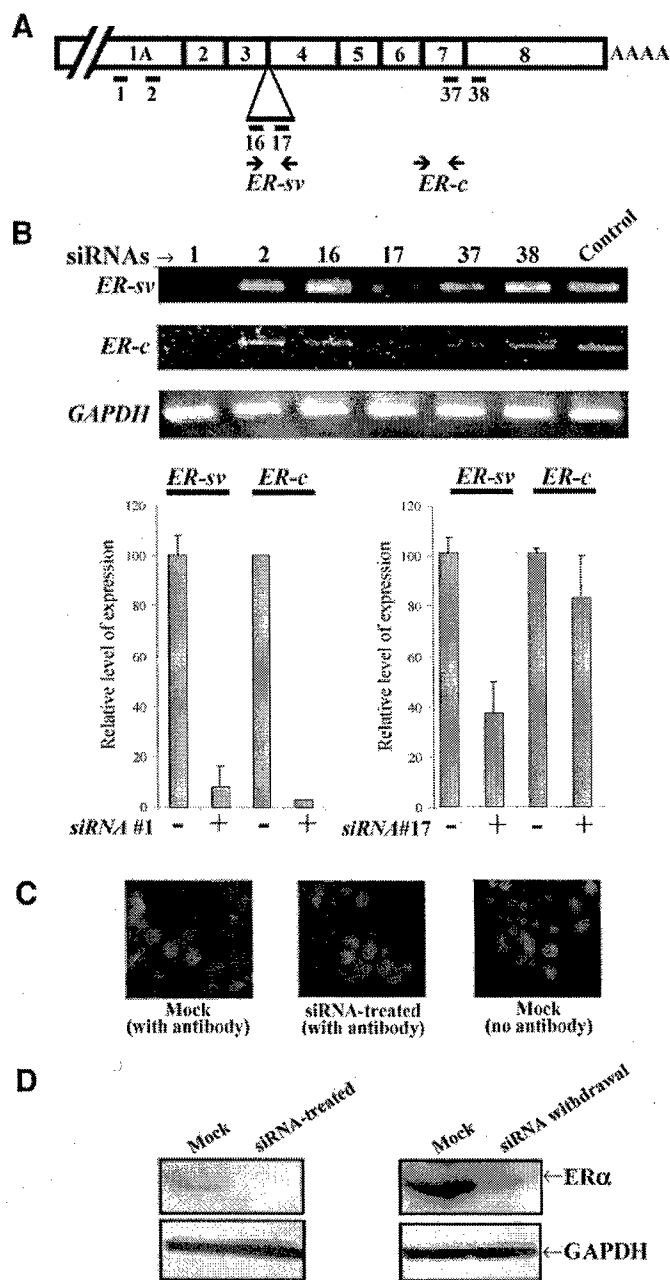

Fig. 1. Down-regulation of *ER*α by siRNAs. MCF-7 ERα-positive human breast cancer cells were transfected with six different double-stranded siRNAs for 4 hours. Cells were left untreated for an additional 24 hours, and total RNA and proteins were then harvested for analysis. Additionally, cells were left untreated for a prolonged period of 3 to 4 weeks (see RNAi withdrawal in *D*), and proteins were harvested for analysis. Mock-treated cells were transfected with vehicle only. *A*, map of *ER*α cDNA. The *ER*α mRNAs were transcribed from several unique first exons and seven other common exons. An additional splice variant (between exons 3 and 4) is also shown. Approximate locations of siRNAs (*1, 2, 16, 17, 37,* and *38*) are indicated by *bars*. *B*, RT-PCR of *ER*α. PCR primers specifically for the splice variant (*ER-sv*) and the common transcripts (*ER-c*) are indicated by *arrows* in *A*. The *GAPDH* transcript was used as a control. The expression levels of *ER-sv* or *ER-c* were normalized against *GAPDH* (*bottom panel*) by real-time PCR. *C*, immunofluorescence analysis of ERα expression. Small interfering RNA 1- or mock-treated MCF-7 cells were cultured on microscope coverslips and incubated with an ERα antibody. Positive nuclei staining (Texas Red) was seen only in mock-treated cells (with antibody), but not in siRNA 1-treated (with antibody) or mock-treated (without antibody) cells. 4',6-Diamidino-2-phenylindole was used to counterstain nuclei (*blue*). *D*, Western blot analysis of ERα expression. Cellular protein products from various treatments were harvested and separated by SDS-PAGE for immunoblot analysis with ERα and GAPDH (loading control) antibodies, respectively. Results are representative of at least three independent experiments.

---

[9] http://www-stat.stanford.edu/~tibs/PAM.

Fig. 2. Loss of estrogen signaling leads to epigenetic silencing of the *PR* gene. *A*, genomic map of the *PR* promoter CpG island. The positions of CpG sites in the genomic sequence are indicated by *thin vertical lines*. The positions of two alternative transcription start sites, *PRA* and *PRB*, respectively, are indicated by *bent arrows*. Potential transcription factor binding sites (AP-1 and Sp1) resulting from a TFSEARCH query (www.cbrc.jp/htbin/nph-tfsearch) are marked by *vertical arrows*. The location of the *PR* promoter fragment used for the ChIP assay and the two regions (MSP1 and MSP2) used for MSP are indicated by *horizontal lines* (see Fig. 3*A*). The region amplified for CO-BRA is *underlined*, and the *two vertical arrows* indicate the interrogating *Taq*I restriction (TCGA) sites (see Fig. 3*C*). *B*, time course inhibition of PR transcripts by siRNA treatment. MCF-7 cells were transfected with ERα siRNA 1 for the indicated time periods (8, 24, and 36 hours) and harvested for real-time RT-PCR. Mock-transfected cells were harvested at the 36 hour time point. Primers were designed to amplify a common region of the two known *PR* transcripts. Relative levels of *PR* transcripts were normalized against that of the *GAPDH* loading control. Results from three independent experiments are shown as means ± SE. *C*, ChIP-PCR assay for activating chromatin modifications on the PR CpG promoter island. Chromatin DNA was immunoprecipitated with antibodies specific for ERα, acetylated histone H3 (acetyl-H3 and/or acetyl-H3-K9), or dimethyl-H3-K4. DNA fragments were amplified with a primer pair located in a *PR* CpG island region (indicated in *A*). The final radiolabeled products were separated on 6% polyacrylamide gels and subjected to autoradiography. *In*, total input; −, without antibody; +, with antibody. *D*, ChIP-PCR assays for repressive chromatin modifications on the PR promoter CpG island region at 36 and 168 hours after ERα siRNA treatment. Antibodies against polycomb repressors (YY-1 and EZH2), histone deacetylase (HDAC1), methyl-CpG binding proteins (MBD2 and MeCP2), and DNA methyltransferases (DMNT1, DNMT3a, and DNMT3b) were used in ChIP-PCR assays. *In*, total input; −, without antibody; +, with antibody.
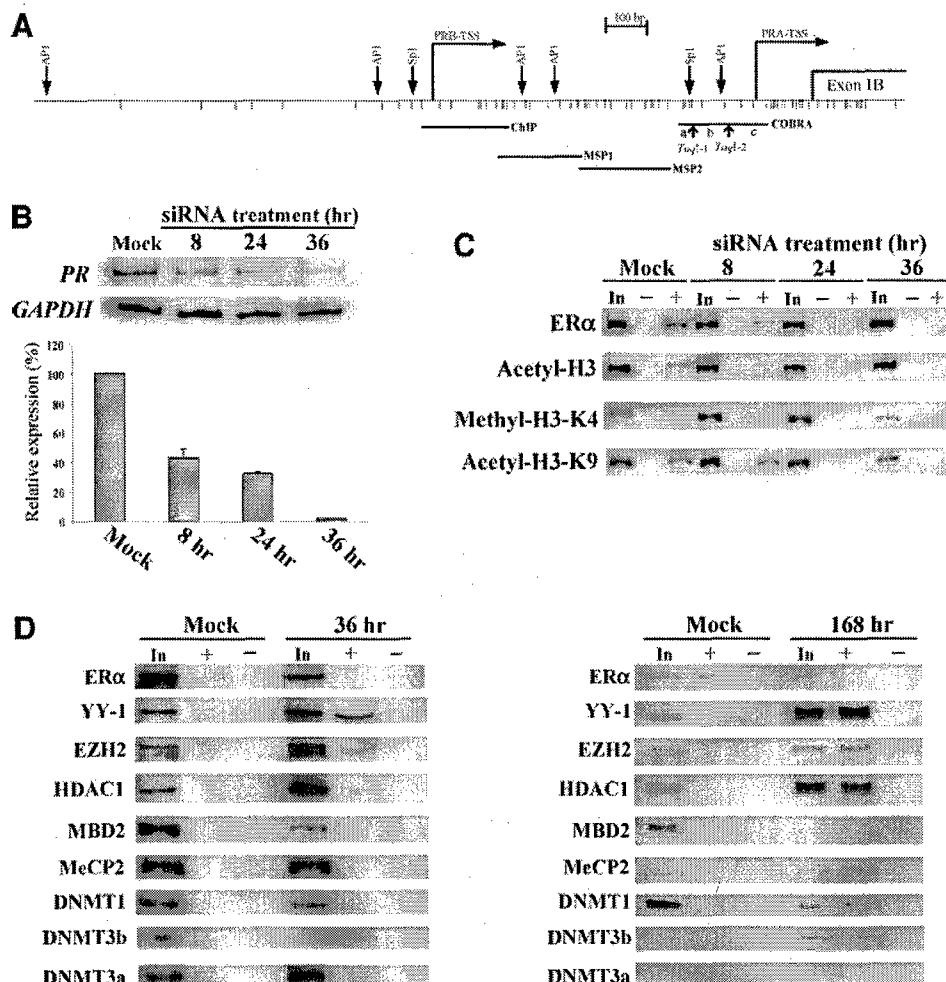
We speculated that this initial transcriptional inactivation might trigger further recruitment of repressor molecules to the *PR* promoter CpG island to subsequently establish a long-term silencing state. ChIP-PCR assays were conducted with a panel of antibodies raised for the polycomb repressors YY-1 and EZH2, histone deacetylase HDAC1, methyl-CpG–binding proteins MBD2 and MeCP2, and DNA methyltransferases DMNT1, DNMT3a, and DNMT3b. At 36 hours after siRNA treatment, YY-1 and EZH2 were bound to the promoter region (Fig. 2*D*). These polycomb proteins have previously been shown to target the regulatory regions of *homeobox* genes, the resulting repression of which can be tissue specific and important for early embryonic development (31, 32). Here we demonstrate for the first time that these proteins have an additional role in repressing an ERα target gene. Furthermore, the *PR* promoter was seen, at 36 hours, to recruit HDAC1 (Fig. 2*D*), a protein known to deacetylate histone protein tails, creating a repressive heterochromatin environment in the targeted promoter area (7, 9, 10). However, at this early time point (36 hours), ChIP-PCR analysis did not detect the presence of the DNA methyltransferase DNMT1 in the *PR* promoter CpG island area (Fig. 2*D*), nor did we observe the presence of MBD2 or MeCP2, which are known to bind methylated CpG sites. Only a faint band corresponding to DNMT3b was detected in the *PR* promoter area by 36 hours after ERα siRNA treatment of MCF-7 cells. Except for DNMT3a, the recruitment of these repressive proteins to the *PR* promoter CpG island was evident by 168 hours after siRNA treatment.

To further determine whether the recruitment of these epigenetic components could trigger *de novo* DNA methylation, MSP assays (33)

were conducted to survey two 5′-end regions of *PR* at different time periods after siRNA treatment. As shown in Fig. 3*A*, *PR* methylation was detected in amplified bisulfite-treated DNA only at 36 hours after treatment. This observation was independently confirmed by conducting semiquantitative COBRA (23). In the assay, ~10% of MCF-7 cells showed methylation in one (Fig. 2*A*, *TaqI-2*) of the two PR *Taq*I sites analyzed 36 hours after siRNA treatment (Fig. 3*B*). Both of these sites became methylated at a later time point (168 hours) of treatment (Fig. 3*B*). This study implies that acquired DNA methylation is a late event and that the density of DNA methylation may gradually accumulate at the 5′-end of *PR* after disrupting ERα signaling by siRNA.

Next, we determined whether this *acquired* promoter methylation could be observed in ERα-negative breast tumors. COBRA was therefore conducted in 32 primary tumors (16 ERα-negative and 16 ERα-positive tumors) and 7 normal controls (see representative examples in Fig. 3*C*). Consistent with the *in vitro* findings, *PR* promoter hypermethylation occurred more frequently in ERα-negative tumors (45%) than in ERα-positive tumors (10%) (χ^2 test, $P < 0.05$).

Reexpression of *PR* Requires Both Estrogen Signal Restoration and DNA Demethylation. The *in vitro* experimental results described above are based on transient siRNA treatment. To determine whether this signal disruption has a lasting impact on *PR* expression, we took advantage of an ERα-negative cell subline, C4-12, derived from ERα-positive MCF-7 cells by long-term hormonal depletion (34). A recent study has indicated that *PR* gene expression is absent in this cell line (35). We therefore examined whether stably reexpressing ERα could restore *PR* gene activity in several established C4-12

Fig. 3. DNA methylation analysis of the *PR* promoter by MSP and COBRA. *A*, bisulfite-treated DNA samples from siRNA- and mock-treated cells were used for amplification with specific primers for MSP1 and MSP2 (see Fig. 2A). Radiolabeled PCR products for unmethylated (*Lanes U*) and methylated (*Lanes M*) DNA strands were separated on 6% polyacrylamide gels. *B*. For COBRA, bisulfite DNA samples from siRNA- and mock-treated cells were amplified and digested with *TaqI* enzyme and then separated on polyacrylamide gels. The digested DNA fragments (*a, b,* and *c*) indicated by the *arrows* reflect methylation of *TaqI* restriction sites within the *PR* promoter CpG island (see Fig. 2A). An *asterisk* indicates PCR artifact or primer-dimer. *C*, COBRA of *PR* promoter in ERα-positive and -negative breast tumors. The percentage of positive methylation was calculated as the intensity of methylated fragments relative to the combined intensity of unmethylated and methylated fragments (*right panel*). All DNA methylation data shown here are representative of at least three independent experiments.
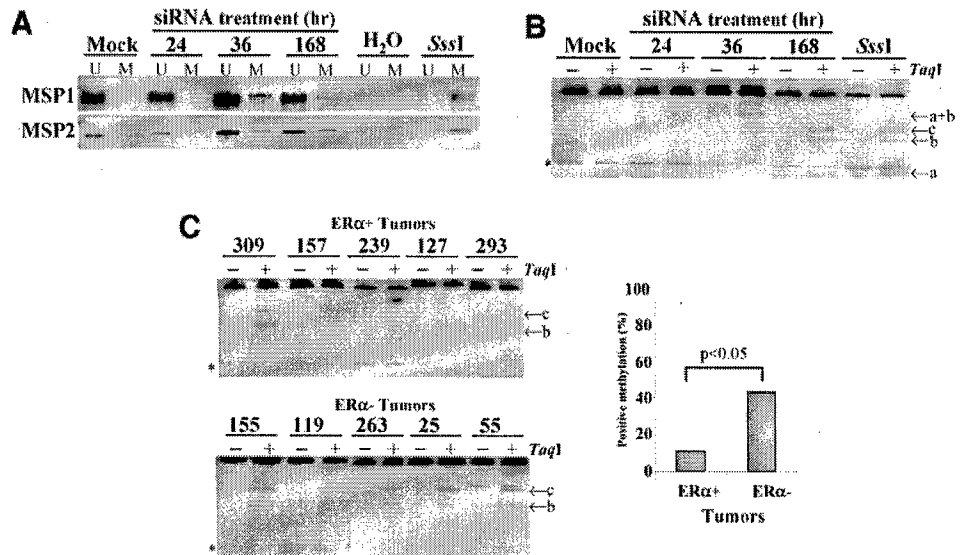
subclones (C4-12/vec, C4-12/ER#1, C4-12/ER#50, and C4-12/ER#86; see examples in Fig. 4*A, inset*).

Treatment of these subclones (*e.g.,* C4-12/ER#86 in Fig. 4*A*) with E_2, however, failed to induce *PR* mRNA expression, demonstrating that reintroduction of ERα alone was insufficient to reactivate expression of a silent *PR* gene. To determine whether loss of *PR* expression was due to DNA methylation, C4-12/vec (*i.e.,* cells stably transfected with empty vector) and C4-12/ER#86 cells were pretreated with 5-AzadC, a DNA demethylating agent, before E_2 treatment. As shown in Fig. 4*A*, sequential treatment with 5-AzadC followed by E_2 resulted in reexpression of *PR* mRNA in C4-12/ER#86 cells, but not in C4-12/vec cells, demonstrating that both ERα expression and DNA demethylation are required to restore PR expression. To further confirm that reactivation of the *PR* gene was due to DNA demethylation, the methylation status of the *PR* promoter CpG island region was examined by MSP (Fig. 4*B*). In contrast to MCF-7 cells in which the

PR promoter CpG island was unmethylated (Fig. 3*A*), methylation was observed in both C4-12/vec and C4-12/ER cells (Fig. 4*B, Lanes 1, 2,* and *5–10*). However, after treatment with 5-AzadC, *PR* promoter methylation was partially reversed in C4-12/vec cells (Fig. 4*B, Lanes 3* and *4*) and completely removed in C4-12/ER#86 cells (Fig. 4*B, Lanes 11* and *12*). Together, these results demonstrate that the silencing of *PR* is maintained, in part, by DNA methylation in the ERα-negative C4-12 cells and that reactivation of the *PR* promoter requires both the presence of ERα and DNA demethylation.

DNA Methylation of Multiple Estrogen Receptor α Downstream Targets Is Triggered by Disrupting Receptor Signaling. To determine whether this epigenetically mediated silencing is a generalized event, we used ChIP-on-chip, a novel microarray-based method developed in our laboratory (36, 37), for a genome-wide screening of ERα downstream targets. In this case, we probed a panel of ~9,000 arrayed CpG island fragments with anti-ERα–coimmuo-

Fig. 4. Treatment of C4-12/ER cells with 5-AzadC restores *PR* mRNA expression. *A*. Expression levels of *PR* mRNA in C4-12/Vec and C4-12/ER cells were determined after treatment with the indicated doses of 5-AzadC for 5 days, followed by 10 nmol/L E_2 for 24 hours. *PR* mRNA levels were measured by quantitative real-time RT-PCR and normalized using β-actin mRNA levels. The results ($X\pm$ SE) are shown from two independent experiments, each in triplicate. ERα expression in C4-12 cells #86 (*A, inset*) was detected by immunoblotting with an anti-ERα antibody. *B*, analysis of *PR* promoter by MSP assay. Bisulfite-treated DNAs from cells treated with or without 5-AzadC were amplified with specific primers for the *PR* promoter CpG island (*i.e.,* the MSP1 region in Fig. 2A). Radiolabeled PCR products for unmethylated (*Lanes U*) and methylated (*Lanes M*) DNA strands were separated on 6% polyacrylamide gels. MSP data shown here are representative of three independent experiments.
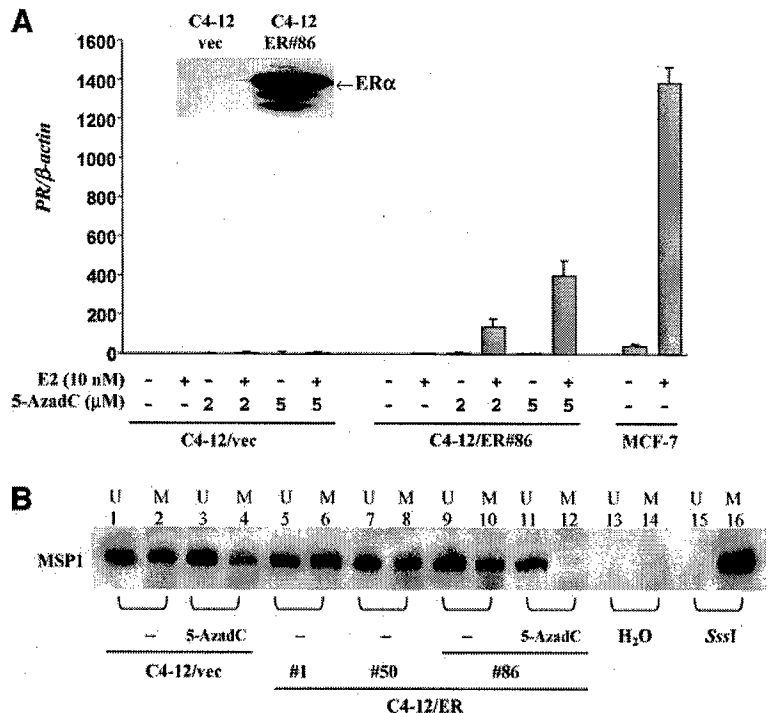
precipitated chromatins. Putative target sequences were used to search for the presence of ERα binding motifs, EREs, and other related binding sites (*e.g.*, AP-1, SP-1, cAMP-responsive element binding protein, and CEBP) by using the Genomatrix[7] and TFSEARCH[8] programs. These computational algorithms identified a total of 70 unique ERα promoter targets, which were used to construct a sub-panel genomic microarray (see a partial list of the genes in Supplementary Table S4). The previously described DMH method (25, 26) was then used to determine the DNA methylation status of these ERα targets in siRNA-treated *versus* mock-treated MCF-7 cells. Amplicons representing genomic pools of methylated DNAs were prepared from these treated cells using our established protocols (25, 26). Cy5 (red dye)- and Cy3 (green dye)-labeled DNAs were prepared from siRNA- and mock-treated cells, respectively, and cohybridized to microscope slides containing the arrayed 70 unique ERα targets. ERα target loci methylated in siRNA-treated cells, but not in mock-treated cells, were expected to show greater Cy5/Cy3 hybridization signals. This is because methylated CpG sites are protected from methylation-sensitive restriction (*i.e.*, HpaII and BstUI) and could thus be amplified by a linker-PCR approach during amplicon preparation. In contrast, unmethylated CpG sites were restricted by the methylation-

sensitive enzymes, could not be amplified by PCR, and were thus devoid of hybridization signals.

To analyze our microarray data, we adapted the "shrunken centroids method" (38) to define the threshold setting for class prediction of methylated ERα target loci. This approach can be used to uniquely define the threshold level that statistically discriminates ERα loci commonly methylated in siRNA-treated cells from the same loci in mock-treated cells. After initial evaluation of the microarray data, we chose the threshold value 2.0 that generates less error ($\leq$0.3) for cross-validation (data not shown). When the cross-validation variances from individual samples were plotted (Fig. 5A), many ERα target loci could be used to discriminate between siRNA-treated cells and mock-treated counterparts (manifested as having many loci with no misclassification error) at the 168 hour time point. However, this threshold level was not sufficiently stringent to discriminate between the mock- and siRNA-treated cell samples at 24 or 36 hours (manifested as having very few loci with low misclassification error). In Fig. 5B, the actual methylation status of individual loci, in comparison with the predicted centroids, is plotted to present an overall change of DNA methylation at different time periods of siRNA treatment. Relative to the overall predicted centroids, a positive value of a locus

Fig. 5. Acquired DNA methylation in multiple ERα downstream targets after estrogen signal disruption. Seventy ERα downstream targets were analyzed by DMH, as described in the text. Fluorescence-labeled methylation amplicons were prepared from siRNA-treated (24, 36, and 168 hours) and mock-treated (168 hours) MCF-7 cells, respectively, and cohybridized to ERα microarray slides. The hybridization output is the measured relative intensity of fluorescence reporter molecules. *A*, test error for different values of shrinkage. Shrunken centroids analysis was conducted using methylation microarray datasets (see detailed description in the text). Tenfold cross-validation was used to estimate the error rate, when a different degree of shrinkage was used to generate the centroids. *B*, Predicted centroids, shown as horizontal units, represent log ratios of DNA methylation. The order of the 70 ERα target loci is arbitrary. Methylation changes were seen only in a few loci at 24 or 36 hours after siRNA treatment; however, a significant methylation change was seen at 168 hours (7 days; $P < 0.05$), displaying positively shrunken values for these 70 loci. *C*, methylation heat map of the 21 selected ERα loci at different time periods after siRNA treatment. These loci were selected because a threshold = 2; error rate $\leq$ 0.3) from cross-validation showed fewer errors in methylation microarray experiments. As shown, DNA methylation of these loci accumulates progressively over time (168 hours) after the siRNA treatment. Data shown here represent three independent microarray experiments. *D*, methylation heat map of the top 12 methylated ERα loci in ERα-negative tumors. Microarray-based DMH was conducted in these clinical samples as described in the text. The derived microarray data were analyzed by the shrunken centroids method.
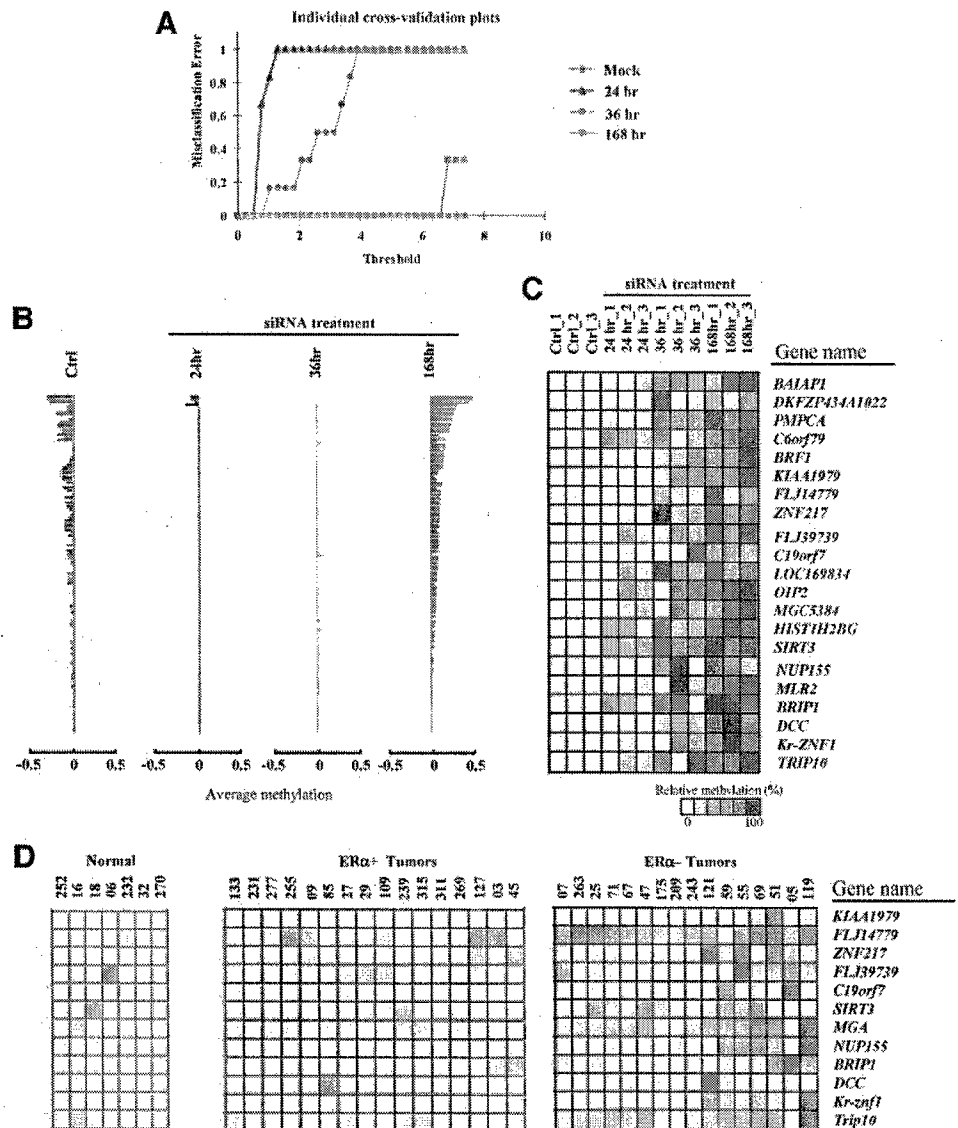
indicates more methylation during the treatment, whereas a negative value indicates less methylation. This shrunken centroids map revealed that *de novo* DNA methylation can be detected in a subset of ERα targets 168 hours after siRNA treatment, but not in cells treated for only 24 or 36 hours after treatment.

To validate the findings of the shrunken centroid analysis, unsupervised cluster analysis was performed on the microarray data, using the top 21 methylated loci selected by machine training ("heat map" shown in Fig. 5C). The result reaffirms the shrunken centroid data in that replicates of each treatment type are clustered together and that the level of methylation increased with the extent of siRNA treatment. A paired *t* test revealed that the methylation status of these 21 loci was significantly different ($P < 0.05$) between the mock-treated (ERα-positive) and siRNA-treated (ERα-negative) cells.

This microarray observation was independently validated by conducting expression and DNA methylation analyses on three newly identified ERα downstream targets, *TRIP10*, *Kr-Znf1*, and *DCC*. In general, the decreased levels of these mRNAs preceded the emergence of DNA methylation at their respective promoter CpG islands (Fig. 6A and B). This epigenetically mediated silencing also indirectly influenced the expression of *MTA3*, a gene known to be regulated via a downstream ERα target and to participate in Mi-2/NuRD nucleosome remodeling (Fig. 6B; ref. 39).

DNA Methylation of ERα Downstream Targets is Preferentially Observed in ERα-Negative Tumors. We next determined whether this *in vitro* finding could be seen *in vivo*. DMH was therefore conducted using the aforementioned 32 primary breast tumors and 7 normal controls. The derived microarray data were then analyzed by the shrunken centroid method. Although the methylation results of these 70 ERα target loci did not clearly segregate tumor samples into subclasses, we observed a general trend that methylated loci appear more frequently in ERα-negative tumors than in ERα-positive tumors ($P < 0.05$). Fig. 5D presents a heat map of the 12 most methylated loci in the studied breast tumors. As shown, we observed higher overall methylation in the ERα-negative tumors (6 of 16 tumors had >40% methylation in the loci analyzed) than in the ERα-positive tumors (only 1 of 16 tumors achieved the same level of methylation). Also, the total number of loci showing DNA methylation was greater in ERα-negative tumors, when compared with ERα-positive tumors. Only four loci showed a low level of methylation in normal breast samples. Methylation analysis by MSP was further conducted for *TRIP10* in these breast samples (Fig. 6C). Consistent with the microarray finding, *TRIP10* promoter hypermethylation was detected in 50% (8 of 16) of ERα-negative tumors but in none of the 16 ERα-positive tumors analyzed (χ^2 test, $P < 0.005$).

DISCUSSION

Understanding the sequence of how complex epigenetic events are established can provide important insights into the molecular mechanisms underlying gene silencing in cancer. However, the "chicken and egg" issue of which comes first, DNA methylation, histone modification, or others, is an ongoing debate in the epigenetic research community. Many early studies of this issue come from non-mammalian systems. Mutations in a histone methyltransferase specific for H3-K9 resulted in loss of DNA methylation in *Neurospora crassa* (15, 16), suggesting that histone methylation can initiate DNA methylation. In *Arabidopsis*, it has been shown that CpNpG methylation depends on a histone H3 methyltransferase (40), also indicating that histone methylation can direct DNA methylation. New evidence suggests that the reverse scenario can occur in heterochromatin (41). In this case, a self-reinforcing system is implemented, allowing for feedback from DNA methylation to histone methylation for the long-
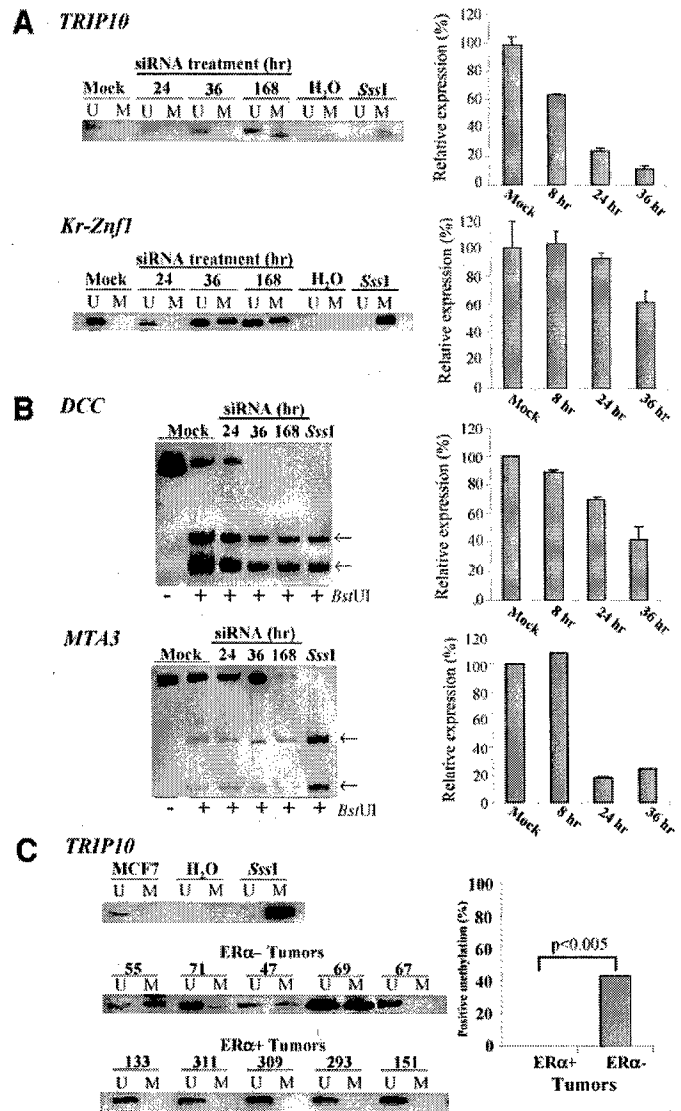

Fig. 6. Methylation and expression analysis of *ERα* target genes. *A.* For methylation-specific PCR assays, bisulfite-treated DNA samples from siRNA- or mock-treated cells were used for amplification with specific primers for *TRIP10* and *Kr-Znf1*, respectively. ^{32}P-labeled PCR products for unmethylated (*Lanes U*) and methylated (*Lanes M*) DNA strands were separated and displayed on 6% polyacrylamide gels (*left panels*). Messenger RNA levels of these genes were measured by quantitative real-time RT-PCR (*right panels*) and normalized using *GAPDH* mRNA expression levels, as described in the text. Results from three independent experiments are shown as means ± SE. The expression level of these genes was significantly reduced by the siRNA treatment (paired *t* test, $P < 0.017$ for *TRIP10* and $P < 0.048$ for *Kr-Znf1*). *B.* For *DCC* and *MTA* genes, COBRA was used to measure DNA methylation. Bisulfite DNA samples were amplified and digested with *Bst*UI enzyme and separated on polyacrylamide gels. The digested DNA fragments shown by *arrows* reflect methylation at the *Bst*UI restriction sites within the *DCC* promoter CpG island (*left panels*). Messenger RNA levels of these genes were measured by quantitative real-time RT-PCR (*right panels*) and normalized using *GAPDH* mRNA expression levels, as described in the text. Results from three independent experiments are shown as means ± SE. The expression level of these genes was significantly reduced by siRNA treatment (paired *t* test, $P < 0.03$ for *DCC* and $P < 0.014$ for *MTA3*). *C.* MSP analysis of the *TRIP10* promoters in 16 ERα-positive and 16 ERα-negative breast tumors. Only representative results are shown.

term maintenance of a heterochromatin state in a gene (41). However, this epigenetic paradigm remains to be explored in mammalian systems. Earlier studies have shown that *in vitro* methylated transgenes can be targets for methyl-CpG–binding proteins, which in turn recruit repressor complexes containing histone deacetylases (17, 18). Fahrner *et al.* (19) suggested that DNA methylation of *hMLH1* can specify unique histone codes for the maintenance of a silenced state. They detected methyl histone 3-lysine 9 in the DNA methylated, transcrip-

tionally silenced promoter CpG island of *hMLH1* in a cancer cell line. Treatment with the DNA demethylating agent 5-AzadC alone, but with not the histone deacetylase inhibitor trichostatin A, resulted in reversal of this repressive histone modification. Taken together, these reports, as well as other studies, imply that in contrast to other organisms, histone modifications may be secondary to DNA methylation in initiating gene silencing in mammalian cells (17, 18, 20, 42).

A study by Bachman *et al.* (43), however, presents a different view with respect to the silencing of the *p16* gene in an experimental system using somatic knockout cells. These authors suggest that chromatin modifications are not totally dependent on prior DNA methylation to initiate gene silencing. In support of this observation, Mutskov and Felsenfeld (44) have recently demonstrated that histone modifications are the primary event associated with the silencing of a transgene, *ILR2*. In this case, a gradual increase in DNA methylation density in and around the *ILR2* promoter was observed after transfection. In contrast to previous observations, these two recent studies therefore suggest that DNA methylation sets up an epigenetic "mark" for the maintenance of long-term silencing, rather than initiating it. Clearly, this epigenetic process is complex and multifaceted, and it is possible that the sequence of epigenetic events for establishing and maintaining the silenced state of a gene can be locus or pathway specific.

The present study suggests that gene inactivation and histone modifications occur before DNA methylation at some ERα target loci. Depicted in Fig. 7 is a hypothetical gene containing an ERE site within the promoter area, the active transcription of which is directly dependent on estrogen signaling. On the removal of this signaling, down-regulation of this gene occurs immediately. Transcriptional repressors (*e.g.*, polycomb proteins) and histone deacetylases are then assembled to its promoter to initiate long-term transcriptional repression. Subsequent recruitment of DNA methyltransferases to the repressor complex methylates CpG sites in the adjacent area. This process may be gradual, with methylation density increasing over time in the targeted area (see the heat map in Fig. 5C). The buildup of DNA

methylation could set up a heritable mark that may eventually replace some of the original repressors to establish a heterochromatin state of long-term silencing. In this case, reactivation of ERα target genes could no longer be achieved by reestablishing estrogen signaling alone (see the example of *PR* in Fig. 4A); it also requires DNA demethylation. In addition to the *PR* gene, we suggest that establishment of epigenetic memory may occur in other critical ERα downstream loci in some breast cancer cells.

The occurrence of DNA methylation in a pathway-specific manner also has a new implication. Altered DNA methylation was originally thought to be a generalized phenomenon arising from a stochastic process in earlier studies (45, 46). This random methylation in tumor suppressor genes at their promoter CpG islands, thus silencing their transcripts, would provide tumor cells with a growth advantage. The specific epigenetic patterns observed in particular cancer types would therefore be derived from clonal selection of the proliferating cells. Some studies (26, 47, 48), however, have indicated that this epigenetic event is not random and that remodeling of the local chromatin structure of a gene may influence its susceptibility to specific DNA methylation. The present study provides some answers to this conundrum. Here we show that dysregulation of normal signaling in cancer cells may result in stable silencing of downstream targets, maintained by epigenetic machinery. This implies that the altered epigenetic condition is pathway specific, rather than a stochastic process in the ERα signaling pathway.

In conclusion, the present study implicates, for the first time, epigenetic influence (*i.e.*, chromatin remodeling and DNA methylation) on transcription of ERα downstream target genes and thus provides a new direction for research in this classical signaling pathway. Unlike irreversible genetic damage, epigenetic alterations are potentially reversible, providing an opportunity for therapeutic intervention in breast cancer. Histone deacetylase inhibitors, alone or together with DNA demethylating agents, may represent novel treatment approaches that could be combined with currently available chemotherapies. Our experimental evidence therefore provides a rationale for such treatment strategies designed to alter aberrant epigenetic processes in hormone-insensitive but receptor-positive breast tumors.

Fig. 7. A proposed model for the epigenetic hierarchy of long-term silencing in *ERα* downstream targets (see further explanation in the text). *HDACs*, histone deacetylases; *DNMTs*, DNA methyltransferases.

REFERENCES

1. Schiff R, Massarweh S, Shou J, Osborne, CK. Breast cancer endocrine resistance: how growth factor signaling and estrogen receptor coregulators modulate response. Clin Cancer Res 2003;9:447s–54s.
2. Jensen EV, Jordan VC. The estrogen receptor: a model for molecular medicine. Clin Cancer Res 2003;9:1980–9.
3. Bird A. DNA methylation patterns and epigenetic memory. Genes Dev 2002; 16:6–21.
4. Ehrlich M. Amount and distribution of 5-methylcytosine in human DNA from different types of tissues or cells. Nucleic Acids Res 1982;10:2709–21.
5. Ehrlich M. Expression of various genes is controlled by DNA methylation during mammalian development. J Cell Biochem 2003;88:899–910.
6. Ballestar E, Esteller M. The impact of chromatin in human cancer: linking DNA methylation to gene silencing. Carcinogenesis (Lond) 2002;23:1103–9.
7. Jones PA, Baylin SB. The fundamental role of epigenetic events in cancer. Nat Rev Genet 2002;3:415–28.
8. Nephew KP, Huang TH-M. Epigenetic gene silencing in cancer initiation and progression. Cancer Lett 2003;190:125–33.
9. Baylin SB, Esteller M, Rountree MR, et al. Aberrant patterns of DNA methylation, chromatin formation and gene expression in cancer. Hum Mol Genet 2001;10: 687–92.
10. Rountree MR, Bachman KE, Herman JG, Baylin SB. DNA methylation, chromatin inheritance, and cancer. Oncogene 2001;20:3156–65.
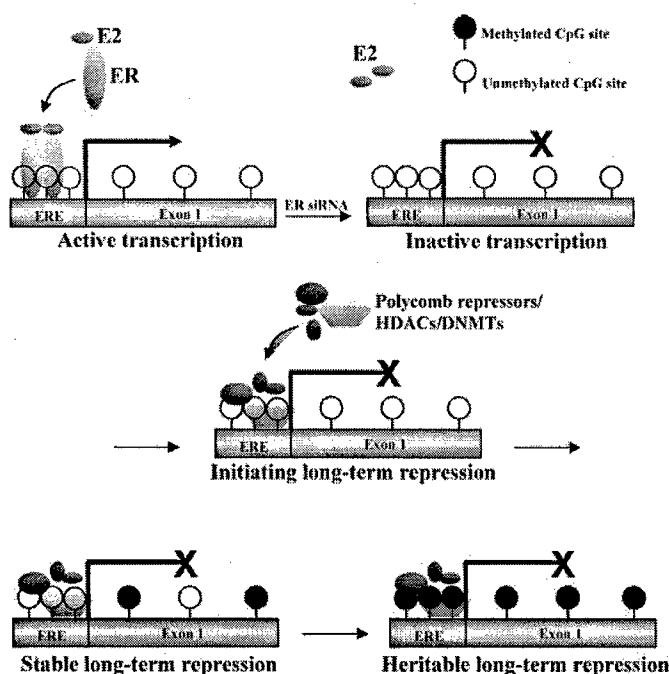
11. Feinberg AP, Tycko B. The history of cancer epigenetics. Nat Rev Cancer 2004;4: 143–53.

12. Jenuwein T, Allis CD. Translating the histone code. Science (Wash DC) 2001;293: 1074–80.

13. Grunstein M. Histone acetylation in chromatin structure and transcription. Nature (Lond) 1997;389:349–52.

14. Kouzarides T. Histone methylation in transcriptional control. Curr Opin Genet Dev 2002;12:198–209.

15. Tamaru H, Selker EU. A histone H3 methyltransferase controls DNA methylation in Neurospora crassa. Nature (Lond) 2001;414:277–83.

16. Tamaru H, Zhang X, McMillen D, et al. Trimethylated lysine 9 of histone H3 is a mark for DNA methylation in Neurospora crassa. Nat Genet 2003;12:177–85.

17. Eden S, Hashimshony T, Keshert I, Cedar H, Thorne AW. DNA methylation models histone acetylation. Nature (Lond) 1998;394:842.

18. Schubeler D, Lorincz MC, Cimbora DM, et al. Genomic targeting of methylated DNA: influence of methylation on transcription, replication, chromatin structure, and histone acetylation. Mol Cell Biol 2000;20:9103–12.

19. Fahrner JA, Eguchi S, Herman JG, Baylin SB. Dependence of histone modifications and gene expression on DNA hypermethylation in cancer. Cancer Res 2002;62: 7213–8.

20. Stirzaker C, Song JZ, Davidson B, Clark SJ. Transcriptional gene silencing promotes DNA hypermethylation through a sequential change in chromatin modifications in cancer cells. Cancer Res 2004;64:3871–7.

21. Yan PS, Rodriguez FJ, Laux DE, et al. Hypermethylation of ribosomal RNA genes in human breast carcinoma. Br J Cancer 2000;82:514–7.

22. Aerts JL, Christiaens MR, Vandekerckhove P. Evaluation of progesterone receptor expression in eosinophils using real-time quantitative PCR. Biochim Biophys Acta 2002;1571:167–72.

23. Laird PW, Xiong Z. COBRA: a sensitive and quantitative DNA methylation assay. Nucleic Acids Res 1997;25:2532–4.

24. Cross SH, Charlton JA, Nan X, Bird AP. Purification of CpG islands using a methylated DNA binding column. Nat Genet 1994;6:236–44.

25. Yan PS, Chen CM, Shi H, et al. Dissecting complex epigenetic alterations in breast cancer using CpG island microarrays. Cancer Res 2001;61:8375–80.

26. Huang TH-M, Perry MR, Laux DE. Methylation profiling of CpG islands in human breast cancer cells. Hum Mol Genet 1999;8:459–70.

27. Elbashir SM, Harborth J, Lendeckel W, et al. Duplexes of 21-nucleotide RNAs mediate RNA interference in cultured mammalian cells. Nature (Lond) 2001;411: 494–8.

28. Elbashir SM, Lendeckel W, Tuschl T. RNA interference is mediated by 21- and 22-nucleotide RNAs. Genes Dev 2001;15:188–200.

29. Brummelkamp TR, Bernards R, Agami R. A system for stable expression of short interfering RNAs in mammalian cells. Science (Wash DC) 2002;296:550–3.

30. Geiman TM, Robertson KD. Chromatin remodeling, histone modification, and DNA methylation: how does it all fit together? J Cell Biochem 2002;2002:117–25.

31. Orlando V. Polycomb, epigenomes, and control of cell identity. Cell 2003;112: 599–606.

32. Satijn DP, Otte AP. Polycomb-group protein complexes: do different complexes regulate distinct targets? Biochim Biophys Acta 1999;1447:1–16.

33. Herman JG, Graff JR, Myohanen S, Nelkin B, Baylin SB. Methylation-specific PCR: a novel PCR assay for methylation status of CpG islands. Proc Natl Acad Sci USA 1996;93:9821–6.

34. Oesterreich S, Zhang P, Guler RL, et al. Re-expression of estrogen receptor alpha in estrogen receptor alpha-negative MCF-7 cells restores both estrogen and insulin-like growth factor-mediated signaling and growth. Cancer Res 2001;16:5771–7.

35. Xu X, Murdoch FE, Curran EM, Welshons WV, Fritsch MK. Transcription factor accessibility and histone acetylation of the progesterone receptor gene differs between parental MCF-7 cells and a subline that has lost progesterone receptor expression. Gene (Amst) 2004;17:143–51.

36. Weinmann AS, Yan PS, Oberley MJ, Huang T H-M, Farnham PJ. Isolating human transcription factor targets by coupling chromatin immunoprecipitation and CpG island microarray analysis. Genes Dev 2002;16:235–44.

37. Shi H, Wei SH, Leu Y-W, et al. Triple analysis of the cancer epigenome: an integrated microarray system for analyzing gene expression. DNA methylation, and histone acetylation. Cancer Res 2003;63:2164–71.

38. Tibshirani R, Hastie T, Narasimhan B, Chu G. Diagnosis of multiple cancer types by shrunken centroids of gene expression. Proc Natl Acad Sci USA 2002;99:6567–72.

39. Fujita N, Jaye DL, Kajita M, et al. MTA3, a Mi-2/NuRD complex subunit, regulates an invasive growth pathway in breast cancer. Cell 2003;113:207–19.

40. Jackson JP, Lindroth AM, Cao X, Jacobsen SE. Control of CpNpG DNA methylation by the KRYPTONITE histone H3 methyltransferase. Nature (Lond) 2002;416: 556–60.

41. Tariq M, Saze H, Probst AV, et al. Erasure of CpG methylation in Arabidopsis alters patterns of histone H3 methylation in heterochromatin. Proc Natl Acad Sci USA 2003;100:8823–7.

42. Lynch CA, Tycko B, Bestor TH, Walsh CP. Reactivation of a silenced H19 gene in human rhabdomyosarcoma by demethylation of DNA but not by histone hyperacetylation. Mol Cancer 2002;1:2.

43. Bachman KE, Park BH, Rhee I, et al. Histone modifications and silencing prior to DNA methylation of a tumor supporessor gene. Cancer Cell 2003;3:89–95.

44. Mutskov V, Felsenfeld G. Silencing of transgene transcription precedes methylation of promoter DNA and histone H3 lysine 9. EMBO J 2004;1:1–12.

45. Jones PA. DNA methylation errors and cancer. Cancer Res 1996;56:2463–7.

46. Pferfer GP, Steigerwald SD, Hansen RS, Gartler SM, Riggs AD. Polymerase chain reaction-aided genomic sequencing of an X chromosome-linked CpG island: methylation patterns suggest clonal inheritance, CpG site autonomy and an explanation of activity state stability. Proc Natl Acad Sci USA 1990;87:8252–6.

47. Feltus FA, Lee EK, Costello JF, Plass C, Vertino PM. Predicting aberrant CpG island methylation. Proc Natl Acad Sci USA 2003;100:12253–8.

48. Costello JF, Fruhwald MC, Smiraglia DJ, et al. Aberrant CpG-island methylation has non-random and tumour-type-specific patterns. Nat Genet 2000;24:132–8.